Downlink Beamforming for Energy-Efficient Heterogeneous Networks With Massive MIMO and Small Cells

5 authors, including:

Some of the authors of this publication are also working on these related projects:

Project The combination of millimeter-wave and non-orthogonal multiple access (mmWave-NOMA) View project

Project Probabilistic Tensor Data Analysis View project

Downlink Beamforming for Energy-Efficient Heterogeneous Networks with Massive MIMO and Small Cells

Long D. Nguyen, Hoang D. Tuan, Trung Q. Duong, Octavia A. Dobre and H. Vincent Poor

Abstract—**A heterogeneous network (HetNet) of a macro-cell base station equipped with a large-scale antenna array (massive MIMO) overlaying a number of small cell base stations (small cells) can provide high quality of service (QoS) to multiple users under low transmit power budget. However, the circuit power for operating such a network, which is proportional to the number of transmit antennas, poses a problem in terms of its energy efficiency. This paper addresses the beamforming design at the base stations to optimize the network energy efficiency under QoS constraints and a transmit power budget. Beamforming tailored for weak, strong and medium cross-tier interference HetNets is proposed. In contrast to the conventional transmit strategy for power efficiency in meeting the users' QoS requirements, which suggests the use of a few hundred antennas, it is found out that the overall network energy efficiency quickly drops if this number exceeds 50. It is found that, for a given number of antennas, HetNet is more energy-efficient than massive MIMO when considering overall energy consumption.**

Index Terms—**Heterogeneous networks, massive MIMO, small cell, beamformer design, energy efficiency, optimization**

I. INTRODUCTION

Massive MIMO [1], [2] and small cell networks [3] are presently envisioned as two key technologies of the emerging generation of communication networks (5G) to support a 1000-fold increase in network capacity. Since each of these technologies alone is not expected to meet both the quality-of-service (QoS) and ubiquitous access requirements for 5G [4], combinations of the former overlaying the latter have attracted considerable research interest [5], [6]. In such heterogeneous networks (HetNets), the small cell base stations (SBSs) serve static and low mobility users (SUEs) to explore their proximity to these users, while the massive MIMO base station (MBS) serves higher mobility users (MUEs) to explore its high coverage area and favored channel characteristics. A main issue of HetNets is to manage both intra-tier interferences

and cross-tier interference between the MBS and SBSs [7], [8]. In [9], the SBSs were proposed to be turned-off if they cause an excessive interference to the MBS. Minimization of the downlink transmit power by multiflow-regularized-zero-forcing beamforming subject to users' QoS constraints was considered in [10], which involves a large-scale semi-definite program of dramatically high computational complexity. The so-called reserve time-division-duplexing of MBS operating in downlink mode while the SBSs operate in uplink mode and vice versa was proposed in [6]. Being free of cross-tier interference, both MBS and SBSs when in downlink are supposed to exploit the cross-tier channel state information (CSI) in suppressing their inter-link interference.

With the irreversible trend of network densification in 5G and beyond [11], [12], a natural concern is its consumed power [13]. To meet the requirement of 1000-fold energy efficiency for new technologies [14], the energy efficiency (EE) in terms of the ratio between the information throughput and consumed power has been introduced as a new figure of merit in assessing communication systems (see, e.g., [15]–[17] and references therein). While achieving lower transmit power in offering better QoS with using more antennas, it should be realized that both MBS and SBSs then consume more circuit powers, which are proportional to the number of their antennas. Since the large-scale analysis [6], [18], which is solely based on arbitrary large numbers of antennas and thus does not control the consumed power, does not readily apply in the EE context, the problem of determining the numbers of base stations, antennas and users in uplink to improve the EE was considered in [19]. As surveyed in [17], so far the main tool for addressing the EE maximization problems is Dinkelbach's procedure of fractional programming [20], even though the objective functions are no longer ratios of concave and convex functions; hence in this case each Dinkelbach's iteration invokes solution of a difficult nonconvex optimization problem, which is not easier than the original optimization problem. Two separated energy-efficient beamforming problems were considered in [21]. The first problem is energy-efficient MBS beamforming under constrained interference to the SBSs' users, while the second problem is the energy-efficient SBS beamforming ignoring the interference from the MBSs. Each stationary point computed in each Dinkelbach's iteration is not necessarily feasible. D.C. (difference of two convex functions) iterations [22] were employed in [23] for computation of the nonconvex optimization problem arisen in each Dinkelbach's iteration for the SBSs under constrained interference to the MBS-tier users. Each

Dinkelbach's iteration in joint power allocation and remote radio head (RRH)/high-power node (HPN) association for heterogeneous cloud radio access networks (H-CRAN) invokes computation of a difficult mixed-integer optimization problem. Each Dinkelbach's iteration in HetNets with fixed service rate constraints [24] invokes computation of a very difficult mixed-combinatorial and nonconvex optimization problem, which is then addressed by semi-definite relaxation.

This paper considers a HetNet of an MBS equipped with a large antenna array overlaying multiple SBSs in serving both MUEs and SUEs. The aim is beamforming design at both the MBS and SBSs to maximize the network EE under the users' QoS constraints. Such design problems under different beam-forming classes are formulated as maximizations of fractional functions subject to convex constraints. Avoiding Dinkelbach's computationally inefficient iterations, path-following computational procedures are developed; these invoke computation of a simple convex program to generate a better feasible point and at least converge to a locally optimal solution. Simulations under different scenarios show that it is important to control the number of the MBS antennas maximizing the network EE, which is indeed in sharp contrast to the spectral efficiency (SE) oriented massive MIMO. Moreover, it is also shown in the paper that indeed underlaid small cells are an effective tool for substantially improving the network EE.

The paper is organized as follows. After the Introduction, Section II is devoted to the EE problem statement. Zero-forcing (ZF) MBS beamforming is addressed in Section III. Section IV considers other beamforming classes. A special class of the ZF MBS and SBS beamforming, with a different solution method, is treated in Section V. Simulation results are presented in Section VI, which is followed by the Conclusions. Some fundamental inequalities used in the paper are provided in the Appendix.

Notation. Boldface uppercase and lowercase letters denote matrices and vectors, respectively. $[x]^+ \triangleq \max\{0, x\}$ for a scalar x. The transpose and conjugate transpose of a matrix $\boldsymbol{X}$ are respectively represented by $\boldsymbol{X}^T$ and $\boldsymbol{X}^H$. $\boldsymbol{I}$ and $\boldsymbol{0}$ stand for identity and zero matrices of appropriate dimensions. $\mathrm{Tr}(.)$ is the trace operator. $||\boldsymbol{x}||$ is the Euclidean norm of a vector $\boldsymbol{x}$ and $||\boldsymbol{X}||$ is the Frobenius norm of a matrix $\boldsymbol{X}$. A complex-valued Gaussian random vector with mean $\bar{\boldsymbol{x}}$ and covariance $\boldsymbol{R_x}$ is denoted by $\boldsymbol{x} \sim \mathcal{CN}(\bar{\boldsymbol{x}}, \boldsymbol{R_x})$. For matrices $\boldsymbol{X}_1, \ldots, \boldsymbol{X}_k$ of appropriate dimension, denote by $[\boldsymbol{X}_1; ...; \boldsymbol{X}_k]$ the matrix $[\boldsymbol{X}_1^T \ \ldots \boldsymbol{X}_k^T]^T$.

II. PROBLEM STATEMENT FOR HETNETS

Consider a HetNet of an MBS of a large-scale N_M antenna array with N_M up to several hundred and S SBSs, which are referred as SBS 1, ..., SBS S. Each SBS s is equipped with N_s antennas. The MBS serves M downlink MUEs, while SBS s serves K_s downlink SUEs within its cell. All users are equipped with a single antenna. For convenience, denote by $\mathcal{K}_M = \{1, \ldots, M\}$ the set of the MUEs and by $\{(s, \ell) | \ell \in \mathcal{K}_s \triangleq \{1, \ldots, K_s\}\}$ the set of those SUEs that are served by SBS s. As Fig. 1 shows, in sharing the same spectrum at the same time, the MBS interferes to all SUEs (s, ℓ), while

TABLE I: Summation of used notations

Notation	Description
N_M	number of MBS antennas
N_s	number of SBS antennas
M	number of users served by MBS (MUEs)
K_s	number of users served by SBS s (SUEs)
$\mathcal{K}_M$	$\{1, \ldots, M\}$
$\mathcal{K}_s$	$\{1, \ldots, K_s\}$
k	an MUE
(s, ℓ)	an SUE served by SBS s
$\mathcal{I}_s$	set of MUEs interfered by SBS s
$\mathcal{N}_k$	set of SBS interfering to MUE k
$\sqrt{\beta_k}\mathbf{h}_k$	channel from MBS to MUE k
$\sqrt{\beta_{s,\ell}}\boldsymbol{\chi}_{s,\ell}$	channel from MBS to SUE (s, ℓ)
$\mathbf{h}_{s,\ell}$	channel from SBS s to SUE (s, ℓ)
$\mathbf{f}_k$	MBS beamforming vector for MUE k
$\mathbf{f}_{s,\ell}$	SBS s' beamforming vector for SUE (s, ℓ)
$\mathbf{F}_M$	set of MBS beamforming vectors
$\mathbf{F}_s$	set of SBS s' beamforming vectors
$\mathbf{F}_S$	$\{\mathbf{F}_s, s = 1, \ldots, S\}$
$\mathbf{F}_{\mathcal{N}_k}$	$\{\mathbf{F}_s, s \in \mathcal{N}_k\}$
$\mathbf{F}$	$\{\mathbf{F}_M, \mathbf{F}_S\}$ (set of all beamforming vectors)
$\tilde{\sigma}_k^{\mathsf{mui}}(\mathbf{F}_M)$	inter-MUE interference to MUE k
$\tilde{\sigma}_{s,\ell}(\mathbf{F}_s)$	inter-SUE interference to SUE (s, ℓ)
$\tilde{\sigma}_{s,\ell}^{\mathsf{mbi}}(\mathbf{F}_M)$	MBS interference to SUE (s, ℓ)
$\tilde{\sigma}_k^{\mathsf{sbi}}(\mathbf{F}\mathcal{N}_k)$	SBS interference to MUE k

the SBSs interfere to those MUEs in their coverage range. Accordingly, $\mathcal{I}_s$ with cardinality I_s is defined as the set of those MUEs that are interfered by SBS s and $\mathcal{N}_k$ is the set of those SBSs that interfere to MUE k.
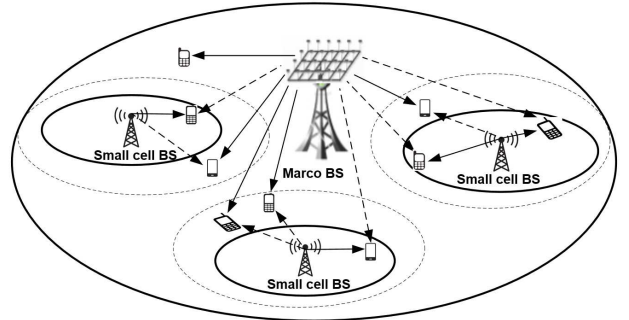

Fig. 1: Illustration to the HetNet. The dash lines denote the interference signals and interference area for SBSs.

Similar to [1], [25] and [18], we will exploit the following structure of the massive MIMO channel from the MBS to the MUEs: $\sqrt{\beta_k}\mathbf{h}_k$, and to the SUEs: $\sqrt{\beta_{s,\ell}}\boldsymbol{\chi}_{s,\ell}$, where $\sqrt{\beta_k}$ and $\sqrt{\beta_{s,\ell}}$ model the path loss and large-scale fading from the MBS to MUE k and SUE (s, ℓ), while $\mathbf{h}_k = (h_{1,k}, ..., h_{N_M,k})^T$ with $h_{mk} \in \mathcal{CN}(0, 1)$ and $\boldsymbol{\chi}_{s,\ell} = (\chi_{1,s,\ell}, \cdots, \chi_{N_M,s,\ell})^T$ with $\chi_{j,s,\ell} \in \mathcal{CN}(0, 1)$ represent the small-scale fading.

The complex baseband signal received by MUE k is

$$y_k = \underbrace{\sqrt{\beta_k} \, \boldsymbol{h}_k^H \boldsymbol{f}_k x_k}_{\text{desired signal}} + \underbrace{\sum_{i \in \mathcal{K}_M \setminus \{k\}} \sqrt{\beta_k} \boldsymbol{h}_k^H \boldsymbol{f}_i x_i}_{\text{inter-MUE (co-tier) interference}}$$

$$+ \underbrace{\sum_{s \in \mathcal{N}_k} \sum_{j=1}^{K_s} \boldsymbol{\eta}_{s,k}^H \boldsymbol{f}_{s,j} x_{s,j}}_{\text{SBS (cross-tier) interference}} + n_k, \qquad (1)$$

where $\mathbf{f}_k \in \mathbb{C}^{N_M}$ and x_k are the beamforming vector and information from the MBS intended to MUE k, respectively, $\boldsymbol{\eta}_{s,k}$ is the channel vector from SBS $s \in \mathcal{N}_k$ to MUE k, $\mathbf{f}_{s,\ell} \in \mathbb{C}^{N_s}$ and $x_{s,\ell}$ are beamforming vector and information from SBS s intended for SUE (s, ℓ), and $n_k \sim \mathcal{CN}(0, \sigma_k^2)$ is the additive white Gaussian noise at MUE k.

The complex baseband signal received by SUE (s, ℓ) is [1]

$$
\begin{aligned}
y_{s,\ell} = \underbrace{\boldsymbol{h}_{s,\ell}^H \boldsymbol{f}_{s,\ell} x_{s,\ell}}_{\text{desired signal}} &+ \underbrace{\sum_{i=1}^{M} \sqrt{\beta_{s,\ell}} \boldsymbol{\chi}_{s,\ell}^H \boldsymbol{f}_i x_i}_{\text{MBS (cross-tier) interference}} \\
&+ \underbrace{\sum_{j' \in \mathcal{K}_s \backslash \{\ell\}} \boldsymbol{h}_{s,\ell}^H \boldsymbol{f}_{s,j'} x_{s,j'}}_{\text{inter-SUE (co-tier) interference}} + n_{s,\ell},
\end{aligned} \tag{2}
$$

where $\mathbf{h}_{s,\ell} \in \mathbb{C}^{N_s}$ is the channel vector and $n_{s,\ell} \sim \mathcal{CN}(0, \sigma_{s,\ell}^2)$ is the additive white Gaussian noise at SUE (s, ℓ).

Let

$$\mathbf{F}_M \triangleq [\mathbf{f}_k]_{k=1,\ldots,M} \in \mathbb{C}^{N_M \times M}, \mathbf{F}_s \triangleq [\mathbf{f}_{s,\ell}]_{\ell=1,\ldots,K_s} \in \mathbb{C}^{N_s \times K_s}$$

and

$$\mathbf{F}_S \triangleq \{\mathbf{F}_s, s = 1, \ldots, S\}, \mathbf{F}_{\mathcal{N}_k} = \{\mathbf{F}_s, s \in \mathcal{N}_k\},$$

$$\mathbf{F} \triangleq \{\mathbf{F}_M, \mathbf{F}_S\}.$$

The network's co-tier interferences are characterized by the inter-MUE and inter-SUE interference functions defined as

$$\widetilde{\sigma}_k^{\mathsf{mui}}(\mathbf{F}_M) \triangleq \beta_k \sum_{i \in \mathcal{K}_M \backslash \{k\}} |\boldsymbol{h}_k^H \boldsymbol{f}_i|^2, k = 1, \ldots, M, \tag{3}$$

and

$$\widetilde{\sigma}_{s,\ell}^{\mathsf{sui}}(\mathbf{F}_s) \triangleq \sum_{j \in \mathcal{K}_s \backslash \{\ell\}} |\boldsymbol{h}_{s,\ell}^H \boldsymbol{f}_{s,j}|^2, \ell = 1, \ldots, K_s; s = 1, \ldots, S, \tag{4}$$

respectively. On the other hand, the network's cross-tier interferences are characterized by the MBS and SBSs interference functions defined as

$$\widetilde{\sigma}_{s,\ell}^{\mathsf{mbi}}(\mathbf{F}_M) \triangleq \beta_{s,\ell} \sum_{i=1}^{M} |\boldsymbol{\chi}_{s,\ell}^H \boldsymbol{f}_i|^2 \tag{5}$$

and

$$\widetilde{\sigma}_k^{\mathsf{sbi}}(\mathbf{F}_{\mathcal{N}_k}) \triangleq \sum_{s \in \mathcal{N}_k} \sum_{j=1}^{K_s} |\boldsymbol{\eta}_{s,k}^H \boldsymbol{f}_{s,j}|^2, k = 1, \ldots, M, \tag{6}$$

respectively.

The information throughputs at MUE k and SUE (s, ℓ) (in nats) are

$$r_k(\mathbf{F}_M, \mathbf{F}_{\mathcal{N}_k}) = \ln \left(1 + \frac{\beta_k |\boldsymbol{h}_k^H \boldsymbol{f}_k|^2}{\widetilde{\sigma}_k^{\mathsf{mui}}(\mathbf{F}_M) + \widetilde{\sigma}_k^{\mathsf{sbi}}(\mathbf{F}_{\mathcal{N}_k}) + \sigma_k^2} \right) \tag{7}$$

and

$$r_{s,\ell}(\mathbf{F}_s, \mathbf{F}_M) = \ln \left(1 + \frac{|\boldsymbol{h}_{s,\ell}^H \boldsymbol{f}_{s,\ell}|^2}{\widetilde{\sigma}_{s,\ell}^{\mathsf{sui}}(\mathbf{F}_s) + \widetilde{\sigma}_{s,\ell}^{\mathsf{mbi}}(\mathbf{F}_M) + \sigma_{s,\ell}^2} \right). \tag{8}$$

The entire consumed power for the downlink transmission can be expressed as

$$P(\mathbf{F}) = P_{\mathsf{mbs}}(\mathbf{F}_M) + \sum_{s=1}^{S} P_s(\mathbf{F}_s), \tag{9}$$

where

$$P_{\mathsf{mbs}}(\mathbf{F}_M) = \alpha \sum_{k=1}^{M} ||\boldsymbol{f}_k||^2 + MP_a + P_c \tag{10}$$

is the power consumed by the MBS and

$$P_s(\mathbf{F}_s) = \alpha_s \sum_{\ell=1}^{K_s} ||\boldsymbol{f}_{s,\ell}||^2 + N_s P_{a,s} + P_{c,s} \tag{11}$$

is the power consumed by SBS s. There, $\alpha > 1$ and $\alpha_s > 1$ are the reciprocal of the drain efficiency of the amplifier of the MBS and SBS s, P_a and $P_{a,s}$ represent the per-antenna circuit power of the MBS and SBS s, and P_c and $P_{c,s}$ are the non-transmission power of the MBS and SBS s, respectively. Accordingly, the total SBSs consumed power is

$$P_{\mathsf{sbs}}(\mathbf{F}_S) = \sum_{s=1}^{S} P_s(\mathbf{F}_s).$$

The EE maximization problem under QoS constraints and power budget is formulated as

$$\max_{\mathbf{F}} \frac{\sum_{k=1}^{M} r_k(\mathbf{F}_M, \mathbf{F}_{\mathcal{N}_k}) + \sum_{s=1}^{S} \sum_{\ell=1}^{K_s} r_{s,\ell}(\mathbf{F}_s, \mathbf{F}_M)}{P_{\mathsf{mbs}}(\mathbf{F}_M) + P_{\mathsf{sbs}}(\mathbf{F}_S)} \tag{12a}$$

$$\text{s.t. } r_k(\mathbf{F}_M, \mathbf{F}_{\mathcal{N}_k}) \geq \bar{r}_k, k = 1, \ldots, M, \tag{12b}$$

$$r_{s,\ell}(\mathbf{F}_s, \mathbf{F}_M) \geq \bar{r}_{s,\ell}, \ell = 1, \ldots, N_s; s = 1, \ldots, S, \tag{12c}$$

$$\sum_{k=1}^{M} ||\mathbf{f}_k||^2 \leq P_M^{\max}, \tag{12d}$$

$$\sum_{\ell=1}^{K_s} ||\boldsymbol{f}_{s,\ell}||^2 \leq P_s^{\max}, s = 1, \ldots, S, \tag{12e}$$

where the constraints (12b)-(12c) set the QoS data rate requirement at each MUE and SUE, and the constraints (12d)-(12e) keep the sum of the transmit power constraints at the MBS and SBSs under predefined budgets.

The paper follows the network centric techniques like Cloud-RAN and cooperative multipoint (CoMP) [28], where the MBS and SBSs cooperate to solve the EE maximization problem (12) in a central manner. The conventional assumption is that full channel state information (CSI) is available for the optimization of problem (12).

The above problem is very complicated due the presence of both intra-tier and cross-tier interferences, and the large dimension N_M of the MBS beamforming vectors $\mathbf{f}_k \in \mathbb{C}^{N_M}$.

---

[1]Note that in (2) we assume that the small cells are sufficiently far apart from each other so that the inter-small-cell interference can be ignored. This is also true for dense small cells where orthogonal frequency division multiplexing is used to allow sufficiently far apart from each other cells to use the same carrier [26], [27].

One can see from (1) and (2) that the MBS contributes a severe interference to all MUEs and SUEs.

The next sections propose computational solutions for (12) by different classes of MBS and SBS beamforming.

III. Zero-forcing inter-MUE interference based beamforming (MZF)

For $\mathbf{H} = [\mathbf{h}_1 \ \mathbf{h}_2 \ ... \ \mathbf{h}_M] \in \mathbb{C}^{N_M \times M}$, which is very tall due to $N_M >> M$, there is the right inverse of the fat matrix $\mathbf{H}^H = [\mathbf{h}_1^H \ ; \mathbf{h}_2^H \ ... \ ; \mathbf{h}_M^H] \in \mathbb{C}^{M \times N_M}$ defined by

$$\bar{\mathbf{F}}_M = \left[\bar{\boldsymbol{f}}_1 \ldots \bar{\boldsymbol{f}}_M \right] = \boldsymbol{H}(\boldsymbol{H}^H\boldsymbol{H})^{-1}, \quad (13)$$

i.e.

$$\begin{aligned} \boldsymbol{I} = \boldsymbol{H}^H \bar{\boldsymbol{F}}_M &= [\boldsymbol{h}_1^H \bar{\boldsymbol{F}}_M; \ldots; \boldsymbol{h}_M^H \bar{\boldsymbol{F}}_M] \\ &= [\boldsymbol{h}_i^H \bar{\boldsymbol{f}}_j]_{(i,j) \in \mathcal{K}_M \times \mathcal{K}_M}. \end{aligned} \quad (14)$$

which means that $\boldsymbol{h}_i^H \bar{\boldsymbol{f}}_i = 1$ and $\boldsymbol{h}_i^H \bar{\boldsymbol{f}}_j = 0$ for $i \neq j$. Using the normalized vectors $\tilde{\boldsymbol{f}}_k \triangleq \bar{\boldsymbol{f}}_k / \|\bar{\boldsymbol{f}}_k\|$, $k = 1, ..., M$, the MBS beamforming vector $\mathbf{f}_k$ is sought in the class of

$$\mathbf{f}_k = p_k \tilde{\boldsymbol{f}}_k, k = 1, \ldots, M \quad (15)$$

to cancel the inter-MUE interference $\tilde{\sigma}_k^{\mathsf{mui}}(\mathbf{F}_M)$ in (3): $\boldsymbol{h}_k^H \tilde{\boldsymbol{f}}_i = \boldsymbol{h}_k^H \bar{\boldsymbol{f}}_i / \|\bar{\boldsymbol{f}}_i\| = 0$ for $i \neq k$.

For $\mathbf{p} = (p_1, ..., p_M)^T \in \mathbb{R}^M$ and

$$\bar{\beta}_k \triangleq \beta_k |\boldsymbol{h}_k^H \tilde{\boldsymbol{f}}_k|^2, \quad (16)$$

the information throughput (in nats) for MUE k in (7) is

$$r_k(p_k, \mathbf{F}_{\mathcal{N}_k}) = \ln(1 + \frac{p_k^2 \bar{\beta}_k}{\sigma_k^2 + \tilde{\sigma}_k^{\mathsf{sbi}}(\mathbf{F}_{\mathcal{N}_k})}), \quad (17)$$

with the SBS interference $\tilde{\sigma}_k^{\mathsf{sbi}}(\mathbf{F}_{\mathcal{N}_k})$ defined from (6), while the consumed power by the MBS transmission defined by (9) is now a quadratic form of $\mathbf{p}$:

$$\pi_{\mathsf{mbs}}(\mathbf{p}) = \alpha \sum_{k=1}^M p_k^2 + M P_a + P_c. \quad (18)$$

The power constraint (12d) is now

$$\sum_{k=1}^M p_k^2 \leq P_M^{\max}, \ p_k \geq 0, \ k = 1, ..., M. \quad (19)$$

The information throughput for SUE (s, ℓ) in (8) is re-expressed by

$$r_{s,\ell}(\mathbf{F}_s, \mathbf{p}) = \ln(1 + \frac{|\mathbf{h}_{s,\ell}^H \boldsymbol{f}_{s,\ell}|^2}{\sigma_{s,\ell}^{\mathsf{mbi}}(\mathbf{p}) + \tilde{\sigma}_{s,\ell}^{\mathsf{sui}}(\mathbf{F}_s) + \sigma_{s,\ell}^2}), \quad (20)$$

where

$$\sigma_{s,\ell}^{\mathsf{mbi}}(\mathbf{p}) \triangleq \beta_{s,\ell} \sum_{i=1}^M p_i^2 \|\boldsymbol{\chi}_{s,\ell}^H \tilde{\boldsymbol{f}}_i\|^2 \quad (21)$$

is the MBS interference function (see (5)), and $\tilde{\sigma}_{s,\ell}^{\mathsf{sui}}(\mathbf{F}_s)$ is the inter-SUE interference function defined from (4).

Under the class of MZF, the EE maximization problem (12) is now expressed by

$$\max_{\mathbf{p}, \mathbf{F}_S} \Phi(\mathbf{p}, \mathbf{F}_S) \triangleq$$

$$\left(\sum_{k=1}^M \ln(1 + \frac{p_k^2 \bar{\beta}_k}{\sigma_k^2 + \tilde{\sigma}_k^{\mathsf{sbi}}(\mathbf{F}_{\mathcal{N}_k})}) \right.$$
$$\left. + \sum_{s=1}^S \sum_{\ell=1}^{K_s} \ln(1 + \frac{|\mathbf{h}_{s,\ell}^H \boldsymbol{f}_{s,\ell}|^2}{\sigma_{s,\ell}^{\mathsf{mbi}}(\mathbf{p}) + \tilde{\sigma}_{s,\ell}^{\mathsf{sui}}(\mathbf{F}_s) + \sigma_{s,\ell}^2}) \right) /$$
$$(\pi_{\mathsf{mbs}}(\mathbf{p}) + P_{\mathsf{sbs}}(\mathbf{F}_S))$$

$$\text{s.t.} \quad (12e), (19), \quad (22a)$$

$$\ln\left(1 + \frac{p_k^2 \bar{\beta}_k}{\sigma_k^2 + \tilde{\sigma}_k^{\mathsf{sbi}}(\mathbf{F}_{\mathcal{N}_k})}\right) \geq \bar{r}_k, k = 1, \ldots, M, \quad (22b)$$

$$\ln\left(1 + \frac{|\mathbf{h}_{s,\ell}^H \boldsymbol{f}_{s,\ell}|^2}{\sigma_{s,\ell}^{\mathsf{mbi}}(\mathbf{p}) + \tilde{\sigma}_{s,\ell}^{\mathsf{sui}}(\mathbf{F}_s) + \sigma_{s,\ell}^2}\right) \geq \bar{r}_{s,\ell},$$
$$\ell = 1, \ldots, K_s; \ s = 1, ..., S. \quad (22c)$$

The nonconvex constraint (22b) is seen equivalent to the following second-order cone (SOC) constraint

$$p_k \sqrt{\bar{\beta}_k} \geq \sqrt{e^{\bar{r}_k} - 1} \sqrt{\sigma_k^2 + \tilde{\sigma}_k^{\mathsf{sbi}}(\mathbf{F}_{\mathcal{N}_k})}, k = 1, \ldots, M. \quad (23)$$

As observed in [29], for $\bar{\boldsymbol{f}}_{s,\ell} \triangleq e^{-\jmath.\arg(\boldsymbol{h}_{s,\ell}^H \boldsymbol{f}_{s,\ell})} \boldsymbol{f}_{s,\ell}$, one has $|\boldsymbol{h}_{s,\ell}^H \boldsymbol{f}_{s,\ell}| = \boldsymbol{h}_{s,\ell}^H \bar{\boldsymbol{f}}_{s,\ell} = \Re\{\boldsymbol{h}_{s,\ell}^H \bar{\boldsymbol{f}}_{s,\ell}\} \geq 0$ in (20). Therefore, $|\boldsymbol{h}_{s,\ell}^H \boldsymbol{f}_{s,\ell}|^2$ in (20) can be equivalently replaced by $(\Re\{\boldsymbol{h}_{s,\ell}^H \boldsymbol{f}_{s,\ell}\})^2$ with $\Re\{\boldsymbol{h}_{s,\ell}^H \boldsymbol{f}_{s,\ell}\} \geq 0, \ell = 1, \ldots, N_s; s = 1, \ldots, S$. Consequently, the nonconvex constraint (22c) is also equivalent to the SOC constraint

$$\Re\{\mathbf{h}_{s,\ell}^H \boldsymbol{f}_{s,\ell}\} \geq \sqrt{(e^{\bar{r}_{s,\ell}} - 1)} \sqrt{\sigma_{s,\ell}^{\mathsf{mbi}}(\mathbf{p}) + \tilde{\sigma}_{s,\ell}^{\mathsf{sui}}(\mathbf{F}_s) + \sigma_{s,\ell}^2},$$
$$\ell = 1, \ldots, K_s; \ s = 1, ..., S. \quad (24)$$

Therefore, the EE maximization problem (22) is a nonconcave function maximization under convex constraints. Our focus now is to handle its objective function. Let $(\mathbf{p}^{(n)}, \mathbf{F}_S^{(n)})$ be a feasible point for (22) found from the $(n-1)$th iteration. Using inequality (69) in the Appendix for

$$x = x_k \triangleq \frac{p_k^2 \bar{\beta}_k}{\sigma_k^2 + \tilde{\sigma}_k^{\mathsf{sbi}}(\mathbf{F}_{\mathcal{N}_k})}, t \triangleq \pi_{\mathsf{mbs}}(\mathbf{p}) + P_{\mathsf{sbs}}(\mathbf{F}_S)$$

and

$$\bar{x} = x_k^{(n)} \triangleq \frac{(p_k^{(n)})^2 \bar{\beta}_k}{\sigma_k^2 + \tilde{\sigma}_k^{\mathsf{sbi}}(\mathbf{F}_{\mathcal{N}_k}^{(n)})},$$
$$\bar{t} = t^{(n)} \triangleq \pi_{\mathsf{mbs}}(\mathbf{p}^{(n)}) + P_{\mathsf{sbs}}(\mathbf{F}_S^{(n)}),$$

yields the following lower bounding approximation for the first term in the objective function in (22a):

$$\frac{\ln\left(1 + \frac{p_k^2 \bar{\beta}_k}{\sigma_k^2 + \tilde{\sigma}_k^{\mathsf{sbi}}(\mathbf{F}_{\mathcal{N}_k})}\right)}{P(\mathbf{p}, \mathbf{F}_S)} \geq$$

$$a_k^{(n)} - b_k^{(n)} \frac{\sigma_k^2 + \tilde{\sigma}_k^{\mathsf{sbi}}(\mathbf{F}_{\mathcal{N}_k})}{\bar{\beta}_k p_k^2} - c_k^{(n)}(\pi_{\mathsf{mbs}}(\mathbf{p}) + P_{\mathsf{sbs}}(\mathbf{F}_S)) \geq$$

$$g_k^{(n)}(\mathbf{p}, \mathbf{F}_S) \quad (25)$$

over the trust region

$$2p_k - p_k^{(n)} > 0, \quad (26)$$

for

$$g_k^{(n)}(\mathbf{p}, \mathbf{F}_S) \triangleq a_k^{(n)} - b_k^{(n)} \frac{\sigma_k^2 + \tilde{\sigma}_k^{\mathsf{sbi}}(\mathbf{F}_{\mathcal{N}_k})}{\bar{\beta}_k p_k^{(n)}(2p_k - p_k^{(n)})}$$
$$- c_k^{(n)}(\pi_{\mathsf{mbs}}(\mathbf{p}) + P_{\mathsf{sbs}}(\mathbf{F}_S)), \quad (27)$$

where

$$0 < a_k^{(n)} \triangleq 2\frac{\ln(1 + x_k^{(n)})}{t^{(n)}} + \frac{x_k^{(n)}}{t^{(n)}(x_k^{(n)} + 1)},$$
$$0 < b_k^{(n)} \triangleq \frac{(x_k^{(n)})^2}{t^{(n)}(x_k^{(n)} + 1)}, \quad (28)$$
$$0 < c_k^{(n)} \triangleq \frac{\ln(1 + x_k^{(n)})}{(t^{(n)})^2}.$$

To address the second term in the objective function in (22a), by substituting

$$x = x_{s,\ell} \triangleq \frac{(\Re\{\mathbf{h}_{s,\ell}^H \boldsymbol{f}_{s,\ell}\})^2}{\sigma_{s,\ell}^{\mathsf{mbi}}(\mathbf{p}) + \tilde{\sigma}_{s,\ell}^{\mathsf{sui}}(\mathbf{F}_s) + \sigma_{s,\ell}^2},$$
$$t \triangleq \pi_{\mathsf{mbs}}(\mathbf{p}) + P_{\mathsf{sbs}}(\mathbf{F}_S)$$

and

$$\bar{x} = x_{s,\ell}^{(n)} \triangleq \frac{(\Re\{\mathbf{h}_{s,\ell}^H \boldsymbol{f}_{s,\ell}^{(n)}\})^2}{\sigma_{s,\ell}^{\mathsf{mbi}}(\mathbf{p}^{(n)}) + \tilde{\sigma}_{s,\ell}^{\mathsf{sui}}(\mathbf{F}_s^{(n)}) + \sigma_{s,\ell}^2},$$
$$\bar{t} = t^{(n)} \triangleq \pi_{\mathsf{mbs}}(\mathbf{p}^{(n)}) + P_{\mathsf{sbs}}(\mathbf{F}_S^{(n)}),$$

into (69) in the Appendix again and using the inequality (72) in the Appendix, we obtain its following lower bounding approximation:

$$\ln\left(1 + \frac{(\Re\{\mathbf{h}_{s,\ell}^H \boldsymbol{f}_{s,\ell}\})^2}{\sigma_{s,\ell}^{\mathsf{mbi}}(\mathbf{p}) + \tilde{\sigma}_{s,\ell}^{\mathsf{sui}}(\mathbf{F}_s) + \sigma_{s,\ell}^2}\right)/P(\mathbf{p}, \mathbf{F}_S) \geq$$
$$a_{s,\ell}^{(n)} - b_{s,\ell}^{(n)} \frac{\sigma_{s,\ell}^{\mathsf{mbi}}(\mathbf{p}) + \tilde{\sigma}_{s,\ell}^{\mathsf{sui}}(\mathbf{F}_s) + \sigma_{s,\ell}^2}{(\Re\{\mathbf{h}_{s,\ell}^H \boldsymbol{f}_{s,\ell}\})^2}$$
$$- c_{s,\ell}^{(n)}(\pi_{\mathsf{mbs}}(\mathbf{p}) + P_{\mathsf{sbs}}(\mathbf{F}_S)) \geq \quad (29)$$
$$g_{s,\ell}^{(n)}(\mathbf{p}, \mathbf{F}_S), \quad (30)$$

for

$$g_{s,\ell}^{(n)}(\mathbf{p}, \mathbf{F}_S) \triangleq$$
$$a_{s,\ell}^{(n)} - b_{s,\ell}^{(n)} \frac{\sigma_{s,\ell}^{\mathsf{mbi}}(\mathbf{p}) + \tilde{\sigma}_{s,\ell}^{\mathsf{sui}}(\mathbf{F}_s) + \sigma_{s,\ell}^2}{2\Re\{\mathbf{h}_{s,\ell}^H \boldsymbol{f}_{s,\ell}^{(n)}\}\Re\{\mathbf{h}_{s,\ell}^H \boldsymbol{f}_{s,\ell}\} - (\Re\{\mathbf{h}_{s,\ell}^H \boldsymbol{f}_{s,\ell}^{(n)}\})^2}$$
$$- c_{s,\ell}^{(n)}(\pi_{\mathsf{mbs}}(\mathbf{p}) + P_{\mathsf{sbs}}(\mathbf{F}_S)) \quad (31)$$

over the trust region

$$2\Re\{\boldsymbol{h}_{s,\ell}^H \boldsymbol{t}_{s,\ell}\} \geq \Re\{\boldsymbol{h}_{s,\ell}^H \boldsymbol{t}_{s,\ell}^{(n)}\}, \ell = 1, \ldots, N_s; \ s = 1, \ldots, S, \quad (32)$$

where

$$0 < a_{s,\ell}^{(n)} \triangleq 2\frac{\ln(1 + x_{s,\ell}^{(n)})}{t^{(n)}} + \frac{x_{s,\ell}^{(n)}}{t^{(n)}(x_{s,\ell}^{(n)} + 1)},$$
$$0 < b_{s,\ell}^{(n)} \triangleq \frac{(x_{s,\ell}^{(n)})^2}{t^{(n)}(x_{s,\ell}^{(n)} + 1)}, \quad (33)$$
$$0 < c_{s,\ell}^{(n)} \triangleq \frac{\ln(1 + x_{s,\ell}^{(n)})}{(t^{(n)})^2}.$$

At the nth iteration, the following convex program is solved to generate the next feasible point $(\mathbf{p}^{(n+1)}, \mathbf{F}_S^{(n+1)})$ for (22):

$$\max_{\mathbf{p}, \mathbf{F}_S} \quad \Phi^{(n)}(\mathbf{p}, \mathbf{F}_S) \triangleq \left[\sum_{k=1}^M g_k^{(n)}(\mathbf{p}, \mathbf{F}_S) + \sum_{s=1}^S \sum_{\ell=1}^{K_s} g_{s,\ell}^{(n)}(\mathbf{p}, \mathbf{F}_s)\right]$$
$$\mathsf{s.t.} \quad (12e), (19), (32), (23), (24), (26). \quad (34)$$

It follows from (25) and (30) that

$$\Phi(\mathbf{p}, \mathbf{F}_S) \geq \Phi^{(n)}(\mathbf{p}, \mathbf{F}_S) \ \forall(\mathbf{p}, \mathbf{F}_S) \quad (35)$$

while it is trivial to check that

$$\Phi(\mathbf{p}^{(n)}, \mathbf{F}_S^{(n)}) = \Phi^{(n)}(\mathbf{p}^{(n)}, \mathbf{F}_S^{(n)}). \quad (36)$$

As $(\mathbf{p}^{(n)}, \mathbf{F}_S^{(n)})$ and $(\mathbf{p}^{(n+1)}, \mathbf{F}_S^{(n+1)})$ are a feasible point and the optimal solution of the convex program (34), respectively, it also follows that

$$\Phi^{(n)}(\mathbf{p}^{(n+1)}, \mathbf{F}_S^{(n+1)}) > \Phi^{(n)}(\mathbf{p}^{(n)}, \mathbf{F}_S^{(n)}), \quad (37)$$

as far as

$$(\mathbf{p}^{(n+1)}, \mathbf{F}_S^{(n+1)}) \neq (\mathbf{p}^{(n)}, \mathbf{F}_S^{(n)}), \quad (38)$$

which together with (35) and (36) yield

$$\Phi(\mathbf{p}^{(n+1)}, \mathbf{F}_S^{(n+1)}) > \Phi(\mathbf{p}^{(n)}, \mathbf{F}_S^{(n)}), \quad (39)$$

showing that $(\mathbf{p}^{(n+1)}, \mathbf{F}_S^{(n+1)})$ is a better feasible point for (22) than $(\mathbf{p}^{(n)}, \mathbf{F}_S^{(n)})$. Thus, in Algorithm 1, we propose a path-following computational procedure for the EE maximization problem (22). An initial point $(\mathbf{p}^{(0)}, \mathbf{F}_S^{(0)})$ for (22) is easily located because all the constraints in (22) are convex. For instance, it can be found from the following convex program:

$$\min_{\mathbf{p}, \mathbf{F}_S} \pi_{\mathsf{mbs}}(\mathbf{p}) + P_{\mathsf{sbs}}(\mathbf{F}_S) \quad \mathsf{s.t.} \quad (12e), (19), (23), (24). \quad (40)$$

Algorithm 1 : Path-following algorithm for solving problem (22)

1: **Initialization**: Choose a feasible point $(\mathbf{p}^{(0)}, \mathbf{F}_S^{(0)})$ for (22). Set $n := 0$.
2: **Repeat**
3:    Solve the problem (34) for its optimal solution $(\mathbf{p}^{(n+1)}, \mathbf{F}_S^{(n+1)})$.
4:    Set $n := n + 1$.
5: **Until** convergence of the objective in (22).

Similar to [30, Prop. 1] we have the following result.

Proposition 1: At least, Algorithm 1 converges to a locally optimal solution of (22) satisfying the Karush-Kuhn-Tucker (KKT) conditions of optimality.

IV. OTHER SCHEMES

The MZF as given by (15) cancels only the inter-MUE interference, under which the MBS interference $\tilde{\sigma}^{\mathsf{mbi}}(\mathbf{F}_M)$ is not controlled. In this section we consider other classes of MBS and SBSs beamforming to enhance both cross-tier and co-tier interferences in optimizing the EE of the system.

A. *Zero forcing co-tier interference based beamforming (*MZF+SZF*)*

In this scheme, referred as MZF+SZF with SZF used as an abbreviation to represent "zero-forcing inter-SUE interference based beamforming", the MBS beamforming vector $\mathbf{f}_k$ is sought in the class of MZF, while the SBS beamforming vector $\mathbf{f}_{s,\ell}$ is designed to force the inter-SUE interference to zero. For each SUE (s,ℓ) define the interfering channel

$$\mathbf{H}_{s,\ell} \triangleq [\mathbf{h}_{s,j}]_{j \in \mathcal{K}_s \setminus \{\ell\}} \in \mathbb{C}^{N_s \times (K_s-1)}, \tag{41}$$

which stacks all channels from SBS s to its SUEs except that to SUE (s,ℓ). To nullify the inter-SUE interference in (4), the following condition must be fulfilled:

$$\mathbf{H}_{s,\ell}^H \boldsymbol{f}_{s,\ell} = \mathbf{0} \in \mathbb{C}^{K_s-1}, \ell = 1,\ldots,K_s, \tag{42}$$

requiring

$$N_s > K_s.$$

Such $\mathbf{f}_{s,\ell}$ is parametrized as

$$\mathbf{f}_{s,\ell} = \boldsymbol{G}_{s,\ell} \boldsymbol{t}_{s,\ell}, \tag{43}$$

where $\boldsymbol{G}_{s,\ell} \in \mathbb{C}^{N_s \times (N_s - K_s + 1)}$ is an orthogonal basis for the null space of $\mathbf{H}_{s,\ell}^H$ and $\boldsymbol{t}_{s,\ell} \in \mathbb{C}^{N_s - K_s + 1}$. Consequently, the information throughput at SUE (s,ℓ) in (8) is

$$r_{s,\ell}^{(2)}(\mathbf{t}_{s,\ell}) = \ln\left(1 + |\bar{\mathbf{h}}_{s,\ell}^H \boldsymbol{t}_{s,\ell}|^2 / (\sigma_{s,\ell}^{\mathsf{mbi}}(\mathbf{p}) + \sigma_{s,\ell}^2)\right) \tag{44}$$

with $\sigma_{s,\ell}^{\mathsf{mbi}}(\mathbf{p})$ defined in (21) and $\bar{\mathbf{h}}_{s,\ell} \triangleq \boldsymbol{G}_{s,\ell}^H \mathbf{h}_{s,\ell}$. For $\boldsymbol{\Theta}_{\ell,k_s} \triangleq \boldsymbol{G}_{s,\ell}^H \boldsymbol{h}_{s,k_s} \in \mathbb{C}^{N_s - K_s + 1}$ and $\mathbf{T}_{\mathcal{N}_k} \triangleq [\mathbf{T}_s]_{s \in \mathcal{N}_k}$, the SBSs interference to MUE k in (6) is

$$\sigma_k^{\mathsf{sbi}}(\mathbf{T}_{\mathcal{N}_k}) \triangleq \widetilde{\sigma}_k^{\mathsf{sbi}}([\mathbf{G}_{s,\ell} \boldsymbol{t}_{s,\ell}]_{s \in \mathcal{N}_k, \ell=1,\ldots,K_s})$$
$$= \sum_{s \in \mathcal{N}_k} \sum_{\ell=1}^{K_s} |\boldsymbol{\Theta}_{\ell,k_s}^H \boldsymbol{t}_{s,\ell}|^2. \tag{45}$$

Now, recalling the definition (21) for the MBS interference to the SUEs, the EE maximization problem is formulated as

$$\max_{\mathbf{p},\mathbf{T}} \frac{\displaystyle\sum_{k=1}^M \ln\left(1 + \frac{p_k^2 \bar{\beta}_k}{\sigma_k^2 + \sigma_k^{\mathsf{sbi}}(\mathbf{T}_{\mathcal{N}_k})}\right)}{\pi(\mathbf{p},\mathbf{T})}$$
$$+ \frac{\displaystyle\sum_{s=1}^S \sum_{\ell=1}^{K_s} \ln\left(1 + \frac{(\Re\{\bar{\mathbf{h}}_{s,\ell}^H \boldsymbol{t}_{s,\ell}\})^2}{\sigma_{s,\ell}^{\mathsf{mbi}}(\mathbf{p}) + \sigma_{s,\ell}^2}\right)}{\pi(\mathbf{p},\mathbf{T})} \tag{46a}$$

s.t. (19),

$$p_k\sqrt{\bar{\beta}_k} \geq \sqrt{e^{\bar{r}_k} - 1}\sqrt{\sigma_k^2 + \sigma_k^{\mathsf{sbi}}(\mathbf{T}_{\mathcal{N}_k})}, k = 1,\ldots,M, \tag{46b}$$

$$\Re\{\bar{\mathbf{h}}_{s,\ell}^H \boldsymbol{t}_{s,\ell}\} \geq \sqrt{(e^{\bar{r}_{s,\ell}} - 1)}\sqrt{\sigma_{s,\ell}^{\mathsf{mbi}}(\mathbf{p}) + \sigma_{s,\ell}^2},$$
$$\ell = 1,\ldots,K_s; \ s = 1,...,S, \tag{46c}$$

$$\sum_{\ell=1}^{K_s} ||\boldsymbol{t}_{s,\ell}||^2 \leq P_s^{\max}, \ s = 1,...,S. \tag{46d}$$

Initialized from a feasible point $(\mathbf{p}^{(0)}, \mathbf{T}^{(0)})$, which is found from the convex program

$$\min_{\mathbf{p},\mathbf{T}} \pi(\mathbf{p},\mathbf{T}) \quad \text{s.t.} \quad (19), (46b), (46c), (46d) \tag{47}$$

at the nth iteration the following convex program is solved to generate the next iterative point $(\mathbf{p}^{(n+1)}, \mathbf{T}^{(n+1)})$ for (46):

$$\max_{\mathbf{p},\mathbf{T}} \left[\sum_{k=1}^M g_k^{(n)}(\mathbf{p},\mathbf{T}) + \sum_{s=1}^S \sum_{\ell=1}^{K_s} f_{s,\ell}^{(n)}(\mathbf{p},\mathbf{T})\right] \tag{48}$$
$$\text{s.t.} \quad (19), (26), (32), (46d), (46b), (46c),$$

where

$$g_k^{(n)}(\mathbf{p},\mathbf{T}) \triangleq a_k^{(n)} - b_k^{(n)} \frac{\sigma_k^2 + \sigma_k^{\mathsf{sbi}}(\mathbf{T}_{\mathcal{N}_k})}{\bar{\beta}_k p_k^{(n)}(2p_k - p_k^{(n)})}$$
$$- c_k^{(n)} \pi(\mathbf{p},\mathbf{T}), \tag{49}$$

with $a_k^{(n)}$, $b_k^{(n)}$ and $c_k^{(n)}$ defined from (28) for

$$x_k^{(n)} \triangleq \frac{(p_k^{(n)})^2 \bar{\beta}_k}{\sigma_k^2 + \sigma_k^{\mathsf{sbi}}(\mathbf{T}_{\mathcal{N}_k}^{(n)})}, t^{(n)} \triangleq \pi(\mathbf{p}^{(n)}, \mathbf{T}^{(n)}),$$

and

$$f_{s,\ell}^{(n)}(\mathbf{p},\mathbf{T}) \triangleq$$
$$a_{s,\ell}^{(n)} - b_{s,\ell}^{(n)} \frac{\sigma_{s,\ell}^{\mathsf{mbi}}(\mathbf{p}) + \sigma_{s,\ell}^2}{2\Re\{\bar{\mathbf{h}}_{s,\ell}^H \boldsymbol{t}_{s,\ell}^{(n)}\}\Re\{\bar{\mathbf{h}}_{s,\ell}^H \boldsymbol{t}_{s,\ell}\} - (\Re\{\bar{\mathbf{h}}_{s,\ell}^H \boldsymbol{t}_{s,\ell}^{(n)}\})^2}$$
$$- c_{s,\ell}^{(n)} \pi(\mathbf{p},\mathbf{T}) \tag{50}$$

with $a_{s,\ell}^{(n)}$, $b_{s,\ell}^{(n)}$ and $c_{s,\ell}^{(n)}$ defined by (33) for

$$x_{s,\ell}^{(n)} \triangleq (\Re\{\bar{\mathbf{h}}_{s,\ell}^H \boldsymbol{t}_{s,\ell}^{(n)}\})^2 / \sigma_{s,\ell}^{\mathsf{mbi}}(\mathbf{p}^{(n)})), t^{(n)} \triangleq \pi(\mathbf{p}^{(n)}, \mathbf{T}^{(n)}).$$

Similar to Proposition 1, it can be easily shown that the computational procedure that invokes the convex program (48) to generate the next iterative point, is path-following for (46), which at least converges to its locally optimal solution satisfying the KKT conditions.

B. *Zero-forcing inter-MUE and MBS and inter-SUE interference beamforming (*ZMI+SZF*)*

In this scheme, referred as ZMI+SZF with ZMI used as an abbreviation to represent "zero-forcing inter-MUE and MBS interferences based beamforming", the MBS beamforming vector $\mathbf{f}_k$ is designed to force both inter-MUE interference and MBS interference to zero, while the SBS beamforming vector $\mathbf{f}_{s,\ell}$ is parametrized by (43) in forcing the inter-SUE interference to zero.

Define the interfering channels from the MBS to the SUEs

$$\boldsymbol{\chi}_s = [\boldsymbol{\chi}_{s,\ell}]_{\ell=1,\ldots,K_s} \in \mathbb{C}^{N_M \times K_s},$$
$$\boldsymbol{\chi} \triangleq [\boldsymbol{\chi}_s]_{s=1,\ldots,S} \in \mathbb{C}^{N_M \times \sum_{s=1}^S K_s}$$

and

$$\boldsymbol{H}_{\mathsf{mbs}} \triangleq [\boldsymbol{H} \ \boldsymbol{\chi}] \in \mathbb{C}^{N_M \times (M + \sum_{s=1}^S K_s)},$$

which is still a very tall as the total number $M + \sum_{s=1}^S K_s$ of users is still small compared to the number N_M of the MBS's antennas. Then the right inverse of the fat matrix $\boldsymbol{H}_{\mathsf{mbs}}^H$ is defined as

$$\bar{\boldsymbol{F}}_{\mathsf{mbs}} = \left[\bar{\mathbf{g}}_1 \cdots \bar{\mathbf{g}}_M \cdots \bar{\mathbf{g}}_{M + \sum_{s=1}^S K_s}\right]$$
$$\triangleq \boldsymbol{H}_{\mathsf{mbs}}(\boldsymbol{H}_{\mathsf{mbs}}^H \boldsymbol{H}_{\mathsf{mbs}})^{-1} \tag{51}$$
$$\in \mathbb{C}^{N_M \times (M + \sum_{s=1}^S K_s)},$$

i.e.,

$$\begin{bmatrix} \mathbf{H}_{\mathsf{mbs}}^H \left[\bar{\mathbf{g}}_1 \dots \bar{\mathbf{g}}_M \right] & \mathbf{H}_{\mathsf{mbs}}^H \left[\bar{\mathbf{g}}_{M+1} \dots \bar{\mathbf{g}}_{M+\sum_{s=1}^S K_s} \right] \end{bmatrix}$$
$$= \mathbf{H}_{\mathsf{mbs}}^H \bar{\boldsymbol{F}}_{\mathsf{mbs}}$$
$$= \mathbf{I} \in \mathbb{R}^{(M+\sum_{s=1}^S K_s) \times (M+\sum_{s=1}^S K_s)}.$$

Particularly,

$$\boldsymbol{H}_{\mathsf{mbs}}^H [\bar{\mathbf{g}}_1 \dots \bar{\mathbf{g}}_M] = \begin{bmatrix} \mathbf{I} \\ \mathbf{O} \end{bmatrix} \in \mathbb{C}^{(M+\sum_{s=1}^S K_s) \times M}.$$

Using the normalized vectors

$$\tilde{\mathbf{f}}_k \triangleq \bar{\mathbf{g}}_k / ||\bar{\mathbf{g}}_k||, k = 1, \dots, M, \tag{52}$$

the MBS beamforming vector $\mathbf{f}_k$ is sough in the class of (15) to nullify the inter-MUE interference and the MBS interference to the SUEs. Under the definition (16) for $\bar{\beta}_k$ with $\tilde{\mathbf{f}}_k$ defined in (52) and the definition (43) for parametrizing beamforming vectors $\mathbf{f}_{s,\ell}$ of SZF, the EE maximization problem (12) is now formulated as

$$\max_{\mathbf{p},\mathbf{T}} \frac{\sum_{k=1}^M \ln\left(1 + p_k^2 \bar{\beta}_k / (\sigma_k^{\mathsf{sbi}}(\mathbf{T}_{\mathcal{N}_k}) + \sigma_k^2)\right)}{\pi(\mathbf{p},\mathbf{T})}$$

$$+ \frac{\sum_{s=1}^S \sum_{\ell=1}^{K_s} \ln\left(1 + (\Re\{\bar{\boldsymbol{h}}_{s,\ell}^H \boldsymbol{t}_{s,\ell}\})^2 / \sigma_{s,\ell}^2\right)}{\pi(\mathbf{p},\mathbf{T})} \tag{53a}$$

$$\text{s.t. } (19), (46b), (46d), \tag{53b}$$

$$\Re\{\bar{\mathbf{h}}_{s,\ell}^H \boldsymbol{t}_{s,\ell}\} \geq \sqrt{(e^{\bar{r}_{s,\ell}} - 1)} \sigma_{s,\ell}, \tag{53c}$$

$$\ell = 1, \dots, K_s; \ s = 1, \dots, S.$$

Initialized from a feasible point $(\mathbf{p}^{(0)}, \mathbf{T}^{(0)})$, which is found from the convex program

$$\min_{\mathbf{p},\mathbf{T}} \pi(\mathbf{p},\mathbf{T}) \quad \text{s.t.} \quad (19), (46b), (46d), (53c) \tag{54}$$

at the nth iteration the following convex program is solved to generate the next iterative feasible point $(\mathbf{p}^{(n+1)}, \mathbf{T}^{(n+1)})$ for (53):

$$\max_{\mathbf{p},\mathbf{T}} \quad [\sum_{k=1}^M g_k^{(n)}(\mathbf{p},\mathbf{T}) + \sum_{s=1}^S \sum_{\ell=1}^{K_s} f_{s,\ell}^{(n)}(\mathbf{p},\mathbf{T})] \tag{55}$$
$$\text{s.t.} \quad (19), (26), (32), (46b), (46d), (53c),$$

where $g_k^{(n)}(\mathbf{p},\mathbf{T})$ is defined in (49), and

$$f_{s,\ell}^{(n)}(\mathbf{p},\mathbf{T}) \triangleq$$

$$a_{s,\ell}^{(n)} - b_{s,\ell}^{(n)} \frac{\sigma_{s,\ell}^{\mathsf{sui}}(\mathbf{T}_s) + \sigma_{s,\ell}^2}{2\Re\{\bar{\boldsymbol{h}}_{s,\ell}^H \boldsymbol{t}_{s,\ell}^{(n)}\}\Re\{\bar{\boldsymbol{h}}_{s,\ell}^H \boldsymbol{t}_{s,\ell}\} - (\Re\{\bar{\boldsymbol{h}}_{s,\ell}^H \boldsymbol{t}_{s,\ell}^{(n)}\})^2}$$
$$- c_{s,\ell}^{(n)} \pi(\mathbf{p},\mathbf{T}), \tag{56}$$

with $a_{s,\ell}^{(n)}, b_{s,\ell}^{(n)}$ and $c_{s,\ell}^{(n)}$ defined by (33) for

$$x_{s,\ell}^{(n)} \triangleq \frac{(\Re\{\bar{\boldsymbol{h}}_{s,\ell}^H \boldsymbol{t}_{s,\ell}^{(n)}\})^2}{\sigma_{s,\ell}^{\mathsf{sui}}(\mathbf{T}_s^{(n)}) + \sigma_{s,\ell}^2}, t^{(n)} \triangleq \pi(\mathbf{p}^{(n)}, \mathbf{T}^{(n)}).$$

Similar to Proposition 1, it can be easily shown that the computational procedure that invokes the convex program

(55) to generate the next iterative point, is path-following for (53), which at least converges to its locally optimal solution satisfying the KKT conditions.

C. Adaptively suppressed co-interference based beamforming (AZMI+SZF)

Denote by $\mathcal{S}_1 = \{1, \dots, S_1\}$ the set of those SBSs that are located sufficiently near to the MBS, and thus, their SUEs are under the strong MBS interference, while denote by $\mathcal{S}_2 = \{S_1+1, \dots, S\}$ the set of those SBSs located far to MBS, and thus, their SUEs are under the weak MBS interference. In this scheme, referred to as AZMI+SZF with AZMI used as an abbreviation to represent "adaptively zero-forcing MBS interference based beamforming", the SBS beamforming vector $\mathbf{f}_{s,\ell}$ is parametrized by (43) to force the inter-SUE interference to zero. On the other hand, the MBS beamforming vector $\mathbf{f}_k$ is designed based on (15) with $\tilde{\mathbf{f}}_k$ defined in (52) with

$$\begin{bmatrix} \bar{\mathbf{g}}_1 \dots \bar{\mathbf{g}}_M \dots \bar{\mathbf{g}}_{M+\sum_{s_1=1}^{S_1} K_{s_1}} \end{bmatrix} \triangleq$$
$$\boldsymbol{H}_{\mathsf{mbs},1}(\boldsymbol{H}_{\mathsf{mbs},1}^H \boldsymbol{H}_{\mathsf{mbs},1})^{-1} \in \mathbb{C}^{N_M \times (M+\sum_{s_1=1}^{S_1} K_{s_1})} \tag{57}$$

and

$$\boldsymbol{\chi}_{s_1} = [\boldsymbol{\chi}_{s_1,\ell}]_{\ell=1,\dots,K_{s_1}} \in \mathbb{C}^{N_M \times K_{s_1}},$$
$$\boldsymbol{\chi}_1 \triangleq [\boldsymbol{\chi}_{s_1}]_{s_1=1,\dots,S_1} \in \mathbb{C}^{N_M \times \sum_{s_1=1}^{S_1} K_{s_1}},$$

$$\boldsymbol{H}_{\mathsf{mbs},1} \triangleq [\boldsymbol{H} \ \boldsymbol{\chi}_1] \in \mathbb{C}^{N_M \times (M+\sum_{s_1=1}^{S_1} K_{s_1})},$$

to nullify the inter-MUE interference and the strong MBS interference to SUEs $(s_1, \ell), s_1 \in \mathcal{S}_1$. The EE maximization problem (12) becomes

$$\max_{\mathbf{p},\mathbf{T}} \frac{\sum_{k=1}^M \ln(1 + \frac{p_k^2 \bar{\beta}_k}{\sigma_k^2 + \sigma_k^{\mathsf{sbi}}(\mathbf{T}_{\mathcal{N}_k})})}{\pi(\mathbf{p},\mathbf{T})}$$

$$+ \frac{\sum_{s=1}^S \sum_{\ell=1}^{K_s} \ln(1 + \frac{(\Re\{\bar{\boldsymbol{h}}_{s,\ell}^H \boldsymbol{t}_{s,\ell}\})^2}{\sigma_{s,\ell}^{\mathsf{mbi}}(\mathbf{p}) + \sigma_{s,\ell}^2})}{\pi(\mathbf{p},\mathbf{T})} \tag{58a}$$

$$\text{s.t. } (19), (46d), \tag{58b}$$

$$p_k \sqrt{\bar{\beta}_k} \geq \sqrt{e^{\bar{r}_k} - 1} \sqrt{\sigma_k^2 + \sigma_k^{\mathsf{sbi}}(\mathbf{T}_{\mathcal{N}_k})}, k = 1, \dots, M, \tag{58c}$$

$$\Re\{\bar{\boldsymbol{h}}_{s,\ell}^H \boldsymbol{t}_{s,\ell}\} \geq \sigma_{s,\ell} \sqrt{e^{\bar{r}_{s,\ell}} - 1},$$
$$\ell = 1, \dots, K_s; s = 1, \dots, S_1, \tag{58d}$$

$$\Re\{\bar{\mathbf{h}}_{s,\ell}^H \boldsymbol{t}_{s,\ell}\} \geq \sqrt{(e^{\bar{r}_{s,\ell}} - 1)} \sqrt{\sigma_{s,\ell}^{\mathsf{mbi}}(\mathbf{p}) + \sigma_{s,\ell}^2},$$
$$\ell = 1, \dots, K_s; \ s = 1, \dots, S_2. \tag{58e}$$

Initialized from a feasible point, which is found from the convex program

$$\min_{\mathbf{p},\mathbf{T}} \pi(\mathbf{p},\mathbf{T}) \quad \text{s.t.} \quad (19), (46d), (58c), (58d), (58e), \tag{59}$$

at the nth iteration, the following convex program is solved to generate a feasible point $(\mathbf{p}^{(n+1)}, \mathbf{T}^{(n+1)})$ for (58):

$$\max_{\mathbf{p},\mathbf{T}} \sum_{k=1}^{M} g_k^{(n)}(\mathbf{p},\mathbf{T}) + \sum_{s=1}^{S}\sum_{\ell=1}^{K_s} f_{s,\ell}^{(n)}(\mathbf{p},\mathbf{T}) \quad \text{(60a)}$$

$$\text{s.t.} \quad (19),(26),(32),(46d),(58c),(58d),(58e), \quad \text{(60b)}$$

where $g_k^{(n)}(\mathbf{p},\mathbf{T})$ is defined in (49), with $a_k^{(n)}$, $b_k^{(n)}$ and $c_k^{(n)}$ from (28), for

$$x_k^{(n)} \triangleq \frac{(p_k^{(n)})^2 \bar{\beta}_k}{\sigma_k^2 + \sigma_k^{\mathsf{sbi}}(\mathbf{T}_{\mathcal{N}_k}^{(n)})}, t^{(n)} \triangleq \pi(\mathbf{p}^{(n)}, \mathbf{T}^{(n)}),$$

and $f_{s,\ell}^{(n)}(\mathbf{p},\mathbf{T})$ is defined from (50), with $a_{s,\ell}^{(n)}$, $b_{s,\ell}^{(n)}$ and $c_{s,\ell}^{(n)}$ from (33), for

$$x_{s,\ell}^{(n)} \triangleq \frac{(\Re\{\bar{\mathbf{h}}_{s,\ell}^H \boldsymbol{t}_{s,\ell}^{(n)}\})^2}{\sigma_{s,\ell}^{\mathsf{mbi}}(\mathbf{p}^{(n)}) + \sigma_{s,\ell}^2}, t^{(n)} \triangleq \pi(\mathbf{p}^{(n)}, \mathbf{T}^{(n)}).$$

Similar to Proposition 1, it can be easily shown that the computational procedure that invokes the convex program (60) to generate the next iterative point, is path-following for (58), which at least converges to its locally optimal solution satisfying the KKT conditions.

V. ENERGY-EFFICIENT ZERO-FORCING HETNET BEAMFORMING (EE ZF)

To show the advantage of HetNets over massive MIMO in terms of the EE, in this section we address the EE maximization problems in the class of zero-forcing beamforming at both MBS and SBSs, i.e. the the BMS beamforming vector $\mathbf{f}_k$ is sought in the class of (15) with $\tilde{\mathbf{f}}_k$ defined from (51) and (52) to cancel both inter-MUE and MBS interferences while the SBS beamforming vector $\mathbf{f}_{s,\ell}$ is also sought to cancel both inter-SUE and SBS interferences as detailed below.

With $\mathbf{H}_s \in \mathbb{C}^{N_s \times I_s}$ defined from (41) and

$$\mathbf{H}_{\mathsf{sbs},s} \triangleq [\, [\mathbf{h}_{s,\ell}]_{\ell=1,...,K_s} \ \mathbf{H}_s \,] \in \mathbb{C}^{N_s \times (K_s + I_s)}$$

the right inverse of $\mathbf{H}_{\mathsf{sbs},s}^H$ is

$$[\bar{\mathbf{f}}_{s,1} \dots \bar{\mathbf{f}}_{s,K_s} \dots \bar{\mathbf{f}}_{s,K_s+I_s}] \triangleq \mathbf{H}_{\mathsf{sbs},s}(\mathbf{H}_{\mathsf{sbs},s}^H \mathbf{H}_{\mathsf{sbs},s})^{-1}.$$

Using the normalized vectors $\tilde{\mathbf{f}}_{s,\ell} = \bar{\mathbf{f}}_{s,\ell}/\|\bar{\mathbf{f}}_{s,\ell}\|$, $\ell = 1,\dots,K_s$, to cancel both inter-SUE and SBS interferences the SUE beamformers $\mathbf{f}_{s,\ell}$ is sought in the form

$$\mathbf{f}_{s,\ell} = p_{s,\ell}\tilde{\mathbf{f}}_{s,\ell}, \ \ell = 1,\dots,N_s; s = 1,\dots,S. \quad \text{(61)}$$

For $\bar{\beta}_k$ defined from (16) and $\bar{\beta}_{s,\ell} \triangleq |\mathbf{h}_{s,\ell}^H \tilde{\mathbf{f}}_{s,\ell}|^2$, while $\mathbf{p}_s \triangleq (p_{s,\ell})_{s=1,\dots,S;\ell=1,\dots,N_s}$, the EE maximization problem (12) is

thus

$$\max_{\mathbf{p},\mathbf{p}_S} \frac{\sum_{k=1}^{M} \ln\left(1 + \bar{\beta}_k p_k^2/\sigma_k^2\right)}{\pi_{\mathsf{mbs}}(\mathbf{p}) + \pi_{\mathsf{sbs}}(\mathbf{p}_S)}$$

$$+ \frac{\sum_{s=1}^{S}\sum_{\ell=1}^{K_s} \ln\left(1 + \bar{\beta}_{s,\ell} p_{s,\ell}^2/\sigma_{s,\ell}^2\right)}{\pi_{\mathsf{mbs}}(\mathbf{p}) + \pi_{\mathsf{sbs}}(\mathbf{p}_S)} \quad \text{(62a)}$$

$$\text{s.t. } (19),$$

$$\ln\left(1 + \bar{\beta}_k p_k^2/\sigma_k^2\right) \geq \bar{r}_k, \ k = 1,\dots,M, \quad \text{(62b)}$$

$$\ln\left(1 + \bar{\beta}_{s,\ell} p_{s,\ell}^2/\sigma_{s,\ell}^2\right) \geq \bar{r}_{s,\ell},$$

$$\ell = 1,\dots,K_s; s = 1,\dots,S, \quad \text{(62c)}$$

$$\sum_{\ell=1}^{K_s} p_{s,\ell}^2 \leq P_s^{\max}, s = 1,..,S, \quad \text{(62d)}$$

where

$$\pi_{\mathsf{sbs}}(\mathbf{p}_S) \triangleq \sum_{s=1}^{S}[\alpha_s \sum_{\ell=1}^{K_s} p_{s,\ell}^2 + N_s P_{a,s} + P_{c,s}].$$

One can see that the objective in (62a) is the ratio of concave and convex functions, for which Dinkelbach's algorithm [20] is applicable. In what follows, we will show that each Dinkelbach's iteration admits a closed-form solution; thus, Dinkelbach's algorithm is very computationally efficient.

First, it follows from (62b) and (62c) that

$$p_k^2 \geq \bar{p}_k := \sigma_k^2(e^{\bar{r}_k} - 1)/\bar{\beta}_k,$$
$$p_{s,\ell}^2 \geq \bar{p}_{s,\ell} := \sigma_{s,\ell}^2(e^{\bar{r}_{s,\ell}} - 1)/\bar{\beta}_{s,\ell}.$$

By making the variable change

$$p_k^2 = \tilde{p}_k + \bar{p}_k, p_{s,\ell}^2 = \tilde{p}_{s,\ell} + \bar{p}_{s,\ell},$$

it is straightforward to solve (62) by applying Dinkelbach's algorithm, which seeks $\tau > 0$ such that the optimal solution of the following optimization problem is zero:

$$\max_{\tilde{\mathbf{p}},\tilde{\mathbf{p}}_S} \sum_{k=1}^{M} \ln\left(a_k + \bar{\beta}_k \tilde{p}_k/\sigma_k^2\right)$$

$$+ \sum_{s=1}^{S}\sum_{\ell=1}^{K_s} \ln\left(a_{s,\ell} + \bar{\beta}_{s,\ell} \tilde{p}_{s,\ell}/\sigma_{s,\ell}^2\right)$$

$$- \tau(\tilde{\pi}_{\mathsf{mbs}}(\tilde{\mathbf{p}}) + \tilde{\pi}_{sbs}(\tilde{\mathbf{p}}_S)) \quad \text{(63a)}$$

$$\text{s.t.} \sum_{k=1}^{M} \tilde{p}_k \leq \bar{P}_M^{\max}, \ \tilde{p}_k \geq 0, \ k = 1,\dots,M, \quad \text{(63b)}$$

$$\sum_{\ell=1}^{K_s} \tilde{p}_{s,\ell} \leq \bar{P}_s^{\max}, s = 1,..,S, \quad \text{(63c)}$$

where $a_k = 1 + \bar{\beta}_k \bar{p}_k/\sigma_k^2$, $\bar{P}_{\mathsf{Mcir}} = \alpha \sum_{k=1}^{M} \bar{p}_k + MP_a + P_c$, $\bar{P}_M^{\max} = P_M^{\max} - \sum_{k=1}^{M} \bar{p}_k$, $\tilde{\pi}_{\mathsf{mbs}}(\tilde{\mathbf{p}}) \triangleq \alpha \sum_{k=1}^{M} \tilde{p}_k + \bar{P}_{\mathsf{Mcir}}$, and $a_{s,\ell} = 1 + \bar{\beta}_{s,\ell} \bar{p}_{s,\ell}/\sigma_{s,\ell}^2$, $\bar{P}_{\mathsf{s,cir}} = \alpha_s \sum_{\ell=1}^{K_s} \bar{p}_{s,\ell} + P_{\mathsf{s,cir}}$, $\bar{P}_s^{\max} = P_s^{\max} - \sum_{\ell=1}^{K_s} \bar{p}_{s,\ell}$, $\tilde{\pi}_{\mathsf{sbs}}(\tilde{\mathbf{p}}_S) \triangleq \sum_{s=1}^{S}[\alpha_s \sum_{\ell=1}^{K_s} \tilde{p}_{s,\ell} + \bar{P}_{\mathsf{s,cir}}]$.

Problem (63) admits the optimal solution in the closed-form:

$$\tilde{p}_k^* = \left[\frac{1}{(\tau\alpha + \lambda_M)} - \frac{a_k \sigma_k^2}{\bar{\beta}_k}\right]^+, k = 1,\dots,M,$$

$$\tilde{p}_{s,\ell}^* = \left[\frac{1}{(\tau\alpha_s + \lambda_s)} - \frac{a_{s,\ell}\sigma_{s,\ell}^2}{\bar{\beta}_{s,\ell}}\right]^+, \quad \text{(64)}$$

$$\ell = 1,\dots,K_s; s = 1,\dots,S,$$

where $\lambda_M = 0$ when

$$\sum_{k=1}^{M} \left[\frac{1}{\tau\alpha} - \frac{a_k \sigma_k^2}{\bar{\beta}_k} \right]^+ \leq \bar{P}_M^{\max}.$$

Otherwise, $\lambda_M > 0$ is located through the bisection method such that

$$\sum_{k=1}^{M} \left[\frac{1}{(\tau\alpha + \lambda_M)} - \frac{a_k \sigma_k^2}{\bar{\beta}_k} \right]^+ = \bar{P}_M^{\max}. \tag{65}$$

Analogously, $\lambda_s = 0$ when

$$\sum_{\ell=1}^{K_s} \left[\frac{1}{\tau\alpha_s} - \frac{a_{s,\ell} \sigma_{s,\ell}^2}{\bar{\beta}_{s,\ell}} \right]^+ \leq \bar{P}_s^{\max}.$$

Otherwise, $\lambda_s > 0$ is located through the bisection method such that

$$\sum_{\ell=1}^{K_s} \left[\frac{1}{(\tau\alpha_s + \lambda_s)} - \frac{a_{s,\ell} \sigma_{s,\ell}^2}{\bar{\beta}_{s,\ell}} \right]^+ = \bar{P}_s^{\max}. \tag{66}$$

The above proposed Dinkelbach's computational procedure for (62) is summarized in Algorithm 2.

Algorithm 2 : Dinkelbach's algorithm for solving problem (62)

1: **Initialization**: Solve (63) for initial $\tau > 0$. If its optimal value is greater than zero, set $\underline{\tau} = \tau$ and reset $\tau \leftarrow 2\tau$ and solve (63) again. Otherwise (its optimal value is lower than zero) set $\bar{\tau} = \tau$. End up by having $\underline{\tau}$ and $\bar{\tau}$ such that the optimal value of (63) is positive for $\tau = \underline{\tau}$ and is negative for $\tau = \bar{\tau}$. The optimal τ for zero optimal value of (63) lies on $[\underline{\tau}, \bar{\tau}]$;
2: **Bisection Method**
3: **Repeat**
4: Solve (63) for $\tau = (\underline{\tau} + \bar{\tau})/2$. If its optimal value is positive, then reset $\underline{\tau} \leftarrow \tau$. Otherwise (its optimal value is negative), reset $\bar{\tau} \leftarrow \tau$.
5: **Until** $\bar{\tau} - \underline{\tau} \leq \epsilon$ (tolerance) to have the optimal value of (63) equal to zero.


VI. NUMERICAL SIMULATIONS

In this section, we evaluate the performance of the proposed algorithms by numerical simulations. Consider a circular cell HetNet with radius 1 km, where the MBS is at the center and $S = 6$ underlaid SBSs are distributed either equally at the cell edge or nearly the MBS, or half of which are equally distributed at the cell edge with another half distributed nearly the MBS as depicted in Fig. 2a, Fig. 2b or Fig. 2c, respectively. These scenarios correspond to weakly coupled, strongly coupled and mixed-coupled HetNets, respectively. The radius of each small cell is 50 m and the radius of the interference area of each SBS is $50 \text{ m} \times 3 = 150 \text{m}$. The MBS is equipped with $N_M > 32$ antennas and each SBS is equipped with $N_s = 4$ antennas. The other simulation parameters are provided in Table I, which follow the prior works [10], [31]. The channel vector $\mathbf{h}_{s,\ell}$ from SBS s in (2) is genereated

by $\sqrt{q_{s,\ell}} \tilde{\mathbf{h}}_{s,\ell}$ with $\sqrt{q_{s,\ell}}$ and $\tilde{\mathbf{h}}_{s,\ell} = (\tilde{\mathbf{h}}_{1,s,\ell}, ..., \tilde{\mathbf{h}}_{N_s,s,\ell})^T$, $\tilde{\mathbf{h}}_{i,s,\ell} \in \mathcal{CN}(0,1)$ representing the path loss and large-scale fading and the small-scale fading, respectively. There are $M = 16$ MUEs with 10 MUEs uniformly distributed outside the SBSs' coverage and each of the remaining 6 MUEs located in the interference area of one of SBSs. Thus, the SBS's interference to the MUEs is the same under these three settings. Each SBS serves two SUEs. The QoS requirement for all users is 0.4 bps/Hz or 4 Mbps [32, Table I].

TABLE II: Simulation Setup

Parameter	Assumption
Carrier frequency / Bandwidth	2 GHz / 10 MHz
MBS transmission power	46 dBm
SBS transmission power	30 dBm
Path loss from MBS to user	$148.1 + 37.6\log_{10} R$ [dB], R in km
Path loss from SBSs to user	$127 + 30\log_{10} R$ [dB], R in km
Shadowing standard deviation	8 dB
Noise power density	-174 dBm/Hz
The power amplifiers parameter	$\alpha_0 = 1/0.388$, $\alpha_s = 1/0.052$
The circuit power per antenna	$P_{a,0}$ = 189 mW, $P_{a,s}$ = 5.6 mW
The non-transmission power	$P_{c,0}$ = 40 dBm, $P_{c,s}$ = 20 dBm
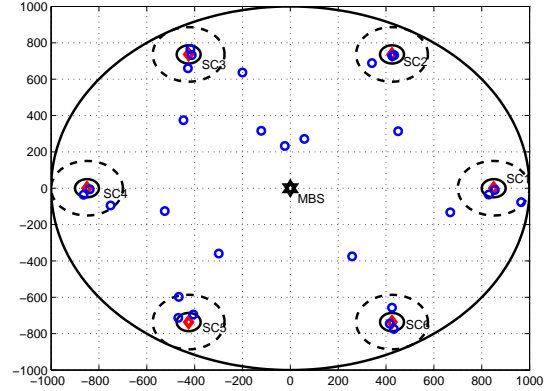
(a) A weakly coupled HetNet
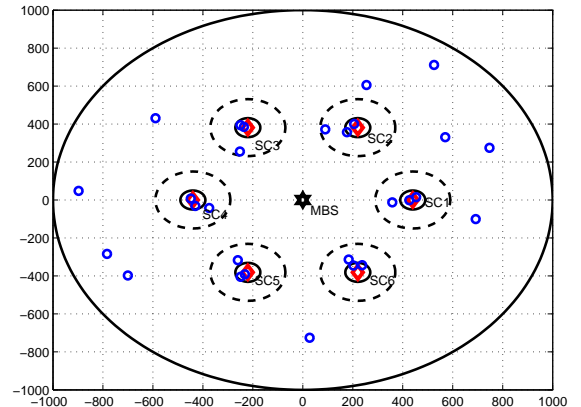
(b) A strongly coupled HetNet
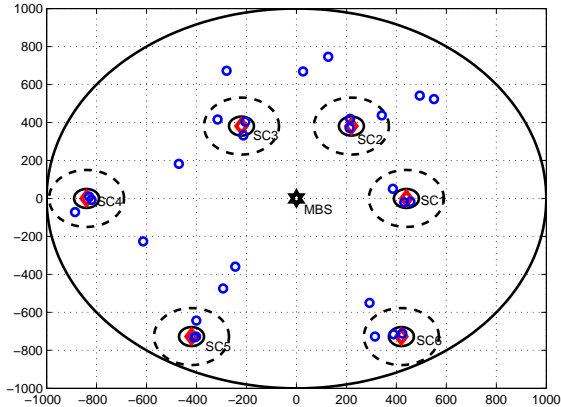
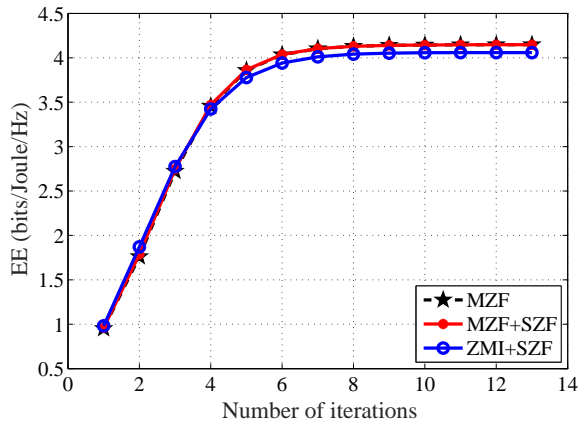(c) A mixed-coupled HetNet

Fig. 2: Three examples of HetNets with different locations of SBSs.

Fig. 4: The EE performance vs. the number of MBS antennas in weakly coupled HetNets. QoS $\bar{r}_k = \bar{r}_{(s,\ell)} \equiv 4$ Mbps.

A. Weakly coupled HetNet

Fig. 3 provides the typical convergence of the proposed path-following computational procedures for solving each particular EE maximization problem in the scenario of weakly coupled HetNets. which is also observed in other scenarios. The EE objective is iteratively increase and converges rapidly within several iterations.

Fig. 3: The convergence vs. iteration number under $N_M = 64$ and QoS $\bar{r}_k = \bar{r}_{(s,\ell)} \equiv 4$ Mbps.

Note that MZF and MZF+SZF use the same class (13), (15) of zero forcing inter-MUE interference MBS beamforming vector $\mathbf{f}_k$ for the EE maximization problems (22) and (46). They achieve the same EE performance but MZF+SZF is obviously more computationally efficient; as such only the curve of MZF+SZF's EE is provided in the next simulations. This observation implies that:

(i) The SBSs' interference to the MUEs can be easily compensated in HetNets without hurting the network's EE, and
(ii) The zero-forcing inter-SUE interference SBS beamforming vector $\mathbf{f}_{s,\ell}$ as parametrized by (43) provides interference enhancement means in HetNets.
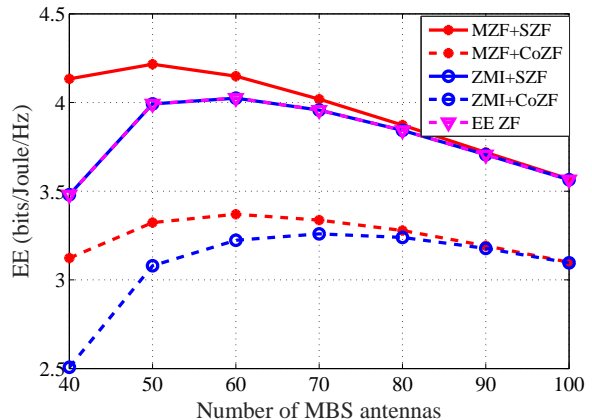
Fig. 4 depicts the EE performance vs. the number N_M of the MBS antennas. Under the weakly coupled scenario, the MBS interference to the SUEs is weak, leaving its cancelation unnecessary. This explains why MZF, which ignores this interference in the EE maximization problem (22), outperforms ZMI+SZF, which nullifies it in the EE maximization problem (53).

The performance gap between MZF and ZMI+SZF is narrower as N_M increases, making the MBS interference stronger. However, there is a huge gap at both $N_M = 40$ and $N_M = 60$, under which either MZF or ZMI+SZF achieves their maximum EE.

It has been shown in [33] that the following conventional SBS beamforming vector $\mathbf{f}_{s,\ell}$ to force the inter-SUE interference to zero is not quite energy-efficient for multi-small-cell networks: $\mathbf{f}_{s,\ell} = p_{s,\ell} \bar{\mathbf{f}}_{s,\ell} / ||\bar{\mathbf{f}}_{s,\ell}||$ with $[\bar{\mathbf{f}}_{s,1} \ldots \bar{\mathbf{f}}_{s,\ell}] = \bar{\mathbf{H}}_s (\bar{\mathbf{H}}_s^H \bar{\mathbf{H}}_s)^{-1}$ and $\bar{\mathbf{H}}_s = [\mathbf{h}_{s,j}]_{j \in \mathcal{K}_s} \in \mathbb{C}^{N_s \times K_s}$, which stacks all channels from SBS s to its SUEs. Figures 4 to 7 also plot the EE by these conventional class of zero-forcing SBS beamforming under different classes of MBS beamforming, which also demonstrates that this conventional zero-forcing SBS beamforming is not energy-efficient for HetNets and is clearly outperformed by the SBS beamforming with beamforming vectors parametrized by (43).
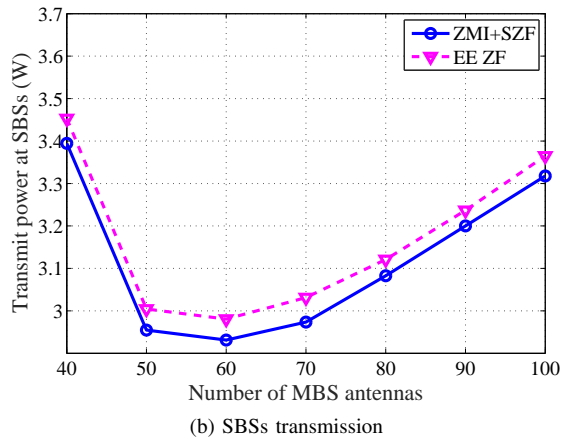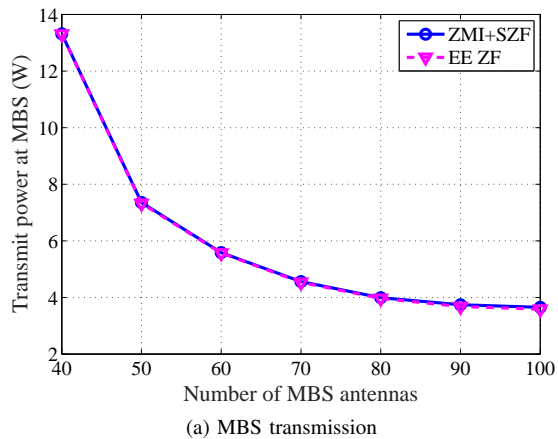
(a) MBS transmission

(b) SBSs transmission

Fig. 5: The transmit power at MBS and SBSs in weakly coupled HetNet.
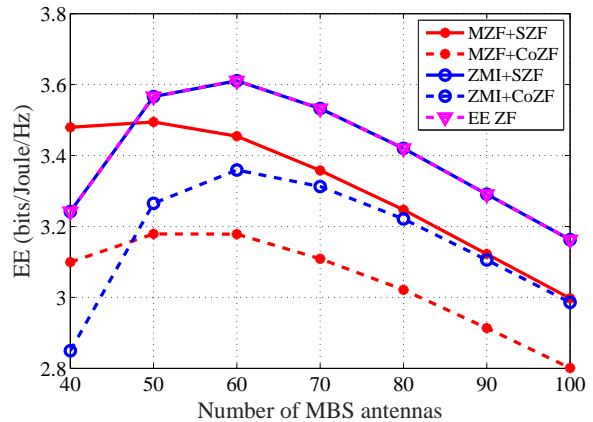
B. Strongly coupled HetNet

Fig. 6: The EE performance vs. the number of MBS antennas in strongly coupled HetNets. QoS $\bar{r}_k = \bar{r}_{(s,\ell)} \equiv 4$ Mbps.

In this scenario, the MBS interference to the SUEs is very strong as all SUEs are located sufficiently near to the MBS. This suggests that the MBS needs to control its interference to make the overall network energy-efficient. However, as Fig. 6 shows, the EE performance achieved by MZF for $N_M = 40$, which ignores this interference while enhancing inter-SUE interference, is almost the same as that achieved by ZMI+SZF, which forces both the MBS interference and inter-SUE interference to zero. This can be explained as the inter-SUE interference enhancement in MZF could still compensate such MBS interference. However, as N_M becomes larger than 40 and the MBS interference becomes too severe, the former cannot compensate the latter and the MZF's performance deteriorates. The zero-forcing the strong MBS interference comes into fruition, making ZMI+SZF easily outperform MZF.

C. Mixed-coupled HetNets

In this scenario, the MBS interference to the SUEs is strong only for the half, which is located sufficiently near to the MBS, and is weak for the other half, which is located far way from the MBS. From the previous results, it is expected that AZMI+SZF, which forces only the strong MBS interference to zero and ignores the weak MBS interference in the EE maximization problem (58), will be efficient. Fig. 7 confirms this intuition. Interestingly, ZMI+SZF and AZMI+SZF achieve their best EE at $N_M = 50$, where their performance gap is clearly visualized.

In summary, the best beamforming strategy is to ignore the interference when it is weak, enhance it when it is medium-strong and cancel it when it is strong. The weak interference does not only make obtaining CSI difficult, but is not needed for optimization either.

On the other hand, observe that ZMI+SZF and EE ZF, which use the same class of MBS beamforming, achieve the same EE. Both schemes particularly force the inter-SUE interference to zero. SBS interference is compensated by MBS beamforming without hurting the network's EE in ZMI+SZF but is nullified by SBS beamforming in EE ZF. Fig. 5 shows that, as expected, the former requires less SBSs' transmission power to optimize the EE than the latter. Furthermore, it also reveals that when the number N_M of the MBS antennas is less than 60, the network's EE is optimised by requiring less transmission power, i.e. the spectral efficiency compensates well the massive MIMO's circuit power. However, when the number N_M is more than 60, the MBS interference becomes the main factor to hurt the network's sum throughput in the numerator of the EE objective. SBSs also need more power to compensate this MBS interference to maintain the QoS requirements.
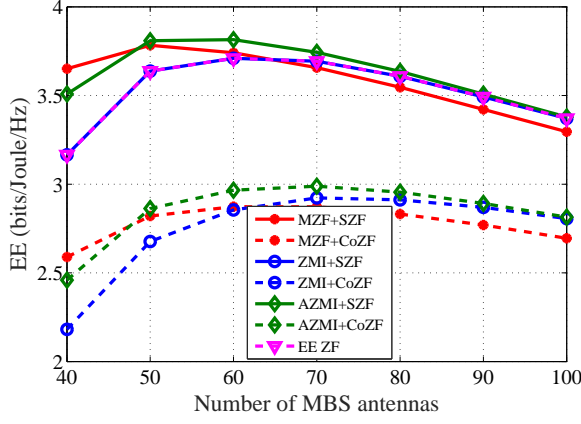
Fig. 7: The EE performance vs. the number of MBS antennas in mixed-coupled HetNets. QoS $\bar{r}_k = \bar{r}_{(s,\ell)} \equiv 4$ Mbps.

D. HetNet EE vs. massive MIMO EE

To have an appropriate setting for EE ZF in the EE optimization problem (62), the number N_s of each SBS antennas is set to 6. The effectiveness of HetNets is demonstrated by comparing its EE performance with that achieved by a massive MIMO with a MBS equipped with $N_M + \sum_{s=1}^{S} N_s$ antennas to serve $M + \sum_{s=1}^{S} K_s$ users in the two following schemes:

- Optimal power allocation for zero-forcing beamforming referred as to MBS PA:

$$\max_{\mathbf{P}} \frac{\sum_{k=1}^{M+\sum_{s=1}^{S} K_s} \ln\left(1 + \bar{\beta}_k p_k^2/\sigma_k^2\right)}{\pi_{\mathsf{mbs}}(\mathbf{p})} \quad (67a)$$

$$\mathsf{s.t.} \quad \sum_{k=1}^{M+\sum_{s=1}^{S} K_s} p_k^2 \leq P_M^{\max}, \quad (67b)$$

$$\ln\left(1 + \bar{\beta}_k p_k^2/\sigma_k^2\right) \geq \bar{r}_k, \quad (67c)$$

$$k = 1, \ldots, (M + \sum_{s=1}^{S} K_s),$$

which is solved by the same Dinkelbach's type algorithm proposed in Section V.

- Equal power allocation for zero-forcing beamforming referred as to MBS EPA with the EE $\left[\sum_{k=1}^{M+\sum_{s=1}^{S} K_s} \ln\left(1 + \bar{\beta}_k p_e^2/\sigma_k^2\right)\right]/\pi_{\mathsf{mbs,EPA}}$, where $p_e = \sqrt{P_M^{\max}/(M + \sum_{s=1}^{S} K_s)}$ is the equal power allocation to all UE and $\pi_{\mathsf{mbs,EPA}} = \alpha P_M^{\max} + P_{\mathsf{Mcir}}$.

In simulations, the proposed Dinkelbach's type algorithm converges within 10 iterations to the optimal solutions in all solved problems.

Fig. 8 shows the significant benefit of using HetNets instead of massive MIMO for the system EE. It can be seen that the EE in massive MIMO is sensitive to the number of users, which are near to the BS (near users). More near users lead to a better EE in massive MIMO. There are many near users in the massive MIMO corresponding to the strongly coupled HetNets. The number of near users in the massive MIMO corresponding to the mixed-coupled HetNets is more than that in the massive MIMO corresponding to the weakly couples

HetNets. On the other hand, the EE in HetNets is dependent on both number of near MUEs and degree of the MBS interference to SUEs. For this reason, the EE is achieved best in the weakly HetNets, second best in the strongly coupled HetNets, and last in the mixed-coupled HetNets. Comparing to the mix-coupled HetNets, the MBS interference is stronger but the number of near MUEs is more so the former still achieve a better EE than the latter.
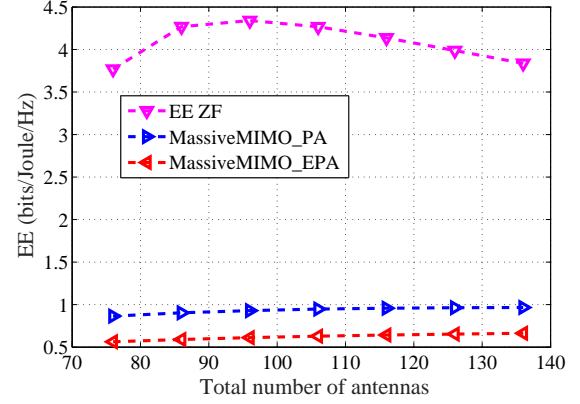
(a) Weakly coupled HetNet
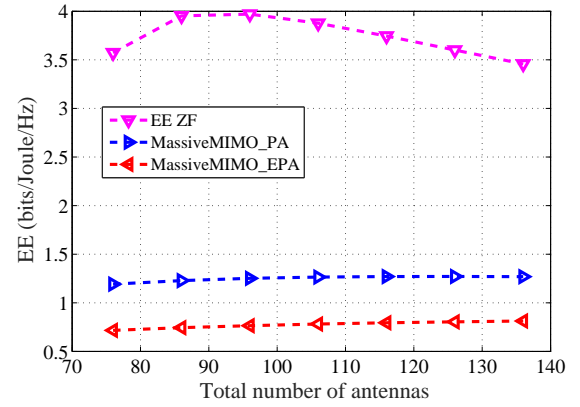
(b) Strongly coupled HetNet
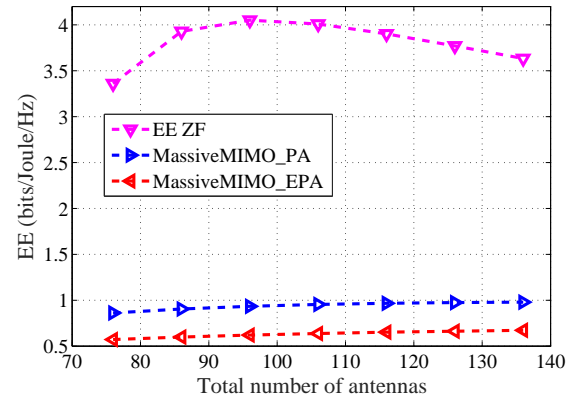
(c) Mixed-coupled HetNet

Fig. 8: The EE performance vs. the number N_M of MBS antennas from 40 to 100 antennas and fixed antennas per SBS with 6 SBSs. The throughput threshold per UE is 4 Mbps.

VII. Conclusions

We have considered various classes of beamforming in HetNets to optimize their energy-efficiency, which is expressed as the ratio of the sum throughput and consumed power. These problems have been formulated as maximizations of highly difficult fractional functions, subject to nonconvex constraints for user QoS satisfaction, and were solved by the proposed path-following algorithms. Numerical examples have shown the efficiency of these algorithms. More importantly, they have shown that in contrast to maximizing the spectral efficiency, which suggests using as many antennas as possible, the EE drops very quickly when this number exceeds 50, which is quite small in the massive MIMO context. HetHets exhibit superior performance in terms of EE when compared with massive MIMO, for a given number of antennas.

Appendix: fundamental inequalities

We exploit the fact that the function $f(x,t) = \frac{\ln(1+1/x)}{t}$ is convex in $x > 0, t > 0$ which can be proved by examining its Hessian. The following inequality for all $x > 0$, $\bar{x} > 0$, $t > 0$ and $\bar{t} > 0$ then holds true [34]:

$$
\begin{aligned}
\frac{\ln(1+1/x)}{t} &\geq f(\bar{x},\bar{t}) + \langle \nabla f(\bar{x},\bar{t}), (x,t) - (\bar{x},\bar{t}) \rangle \\
&= 2\frac{\ln(1+1/\bar{x})}{\bar{t}} + \frac{1}{\bar{t}(\bar{x}+1)} \\
&\quad - \frac{x}{(\bar{x}+1)\bar{x}\bar{t}} - \frac{\ln(1+1/\bar{x})}{\bar{t}^2}t, \quad (68)
\end{aligned}
$$

where ∇ is the gradient operation.

By replacing $1/x \to x$ and $1/\bar{x} \to \bar{x}$ in (68), we have

$$
\frac{\ln(1+x)}{t} \geq a - \frac{b}{x} - ct, \quad (69)
$$

where

$$
a = 2\frac{\ln(1+\bar{x})}{\bar{t}} + \frac{\bar{x}}{\bar{t}(\bar{x}+1)} > 0, b = \frac{\bar{x}^2}{\bar{t}(\bar{x}+1)} > 0,
$$
$$
c = \frac{\ln(1+\bar{x})}{\bar{t}^2} > 0.
$$

By replacing $|x|^2 \to x$ and $|\bar{x}|^2 \to \bar{x}$ in (69) we have

$$
\begin{aligned}
\frac{\ln(1+|x|^2)}{t} &\geq \bar{a} - \frac{\bar{b}}{|x|^2} - \bar{c}t \\
&\geq \bar{a} - \frac{\bar{b}}{2\Re\{x\bar{x}^*\} - |\bar{x}|^2} - \bar{c}t \quad (70)
\end{aligned}
$$

over the trust region

$$
2\Re\{x\bar{x}^*\} - |\bar{x}|^2 > 0, \quad (71)
$$

where

$$
\bar{a} = 2\frac{\ln(1+|\bar{x}|^2)}{\bar{t}} + \frac{|\bar{x}|^2}{\bar{t}(|\bar{x}|^2+1)} > 0,
$$
$$
\bar{b} = \frac{|\bar{x}|^4}{\bar{t}(|\bar{x}|^2+1)} > 0,
$$
$$
\bar{c} = \frac{\ln(1+|\bar{x}|^2)}{\bar{t}^2} > 0.
$$

Finally, we also have the following inequality

$$
\frac{x^2}{t} \geq 2\frac{\bar{x}x}{\bar{t}} - \frac{\bar{x}^2}{\bar{t}^2}t \quad \forall\, x > 0,\ \bar{x} > 0, t > 0, \bar{t} > 0. \quad (72)
$$

References

[1] F. Rusek et al., "Scaling up MIMO: Opportunities and challenges with very large arrays," *IEEE Signal Process. Mag.*, vol. 30, no. 1, pp. 40–60, Jan. 2013.

[2] E. G. Larsson, O. Edfors, F. Tufvesson, and T. L. Marzetta, "Massive MIMO for next generation wireless systems," *IEEE Commun. Mag.*, vol. 52, no. 2, pp. 186–195, Feb. 2014.

[3] J. Hoydis, M. Kobayashi, and M. Debbah, "Green small-cell networks," *IEEE Veh. Technol. Mag.*, vol. 6, no. 1, pp. 37–43, Jan. 2011.

[4] V. Jungnickel et al, "The role of small cells, coordinated multipoint, and massive MIMO in 5G," *IEEE Commun. Mag.*, vol. 52, no. 5, pp. 44–51, May 2014.

[5] J. Hoydis, K. Hosseini, S. t. Brink, and M. Debbah, "Making smart use of excess antennas: Massive MIMO, small cells, and TDD," *Bell Labs Technical J.*, vol. 18, no. 2, pp. 5–21, Apr. 2013.

[6] L. Sanguinetti, A. L. Moustakas, and M. Debbah, "Interference management in 5G reverse TDD HetNets with wireless backhaul: a large system analysis," *IEEE J. Sel. Areas. Commun.*, vol. 33, no. 6, pp. 1187–1200, Jun. 2015.

[7] A. Ghosh et al, "Heterogeneous cellular networks: from theory to practice," *IEEE Commun. Mag.*, vol. 50, no. 6, pp. 54–64, Jun. 2012.

[8] H. S. Dhillon, M. Kountouris, and J. G. Andrews, "Downlink MIMO HetNets: Modeling, ordering results and performance analysis," *IEEE Trans. Wireless Commun.*, vol. 12, no. 10, pp. 5208–5222, Oct. 2013.

[9] A. Adhikary, H. S. Dhillon, and G. Caire, "Massive-MIMO Meets HetNet: Interference coordination through spatial blanking," *IEEE J. Sel. Areas. Commun.*, vol. 33, no. 6, pp. 1171–1186, Jun. 2015.

[10] E. Bjornson, M. Kountouris, and M. Debbah, "Massive MIMO and small cells: improving energy efficiency by optimal soft-cell coordination," in *ICT*, May 2013, pp. 1–5.

[11] N. Bhushan et al, "Network densification: the dominant theme for wireless evolution into 5G," *IEEE Commun. Mag.*, vol. 52, no. 2, pp. 82–89, Feb. 2014.

[12] J. G. Andrews, X. Zhang, G. D. Durgin, and A. K. Gupta, "Are we approaching the fundamental limits of wireless network densification?" *IEEE Commun. Mag.*, vol. 54, no. 10, pp. 184–190, Oct. 2016.

[13] A. Fehske, G. Fettweis, J. Malmodin, and G. Biczok, "The global footprint of mobile communications: The ecological and economic perspective," *IEEE Commun. Mag.*, vol. 49, no. 8, pp. 55–62, Aug. 2011.

[14] GreenTouch Green Meter Research Study, "Reducing the net energy consumption in communications networks by up to 90% by 2020 (version 1.0)," *https://s3-us-west-2.amazonaws.com/belllabs-microsite-greentouch/*, Jun. 2013.

[15] C. Isheden, Z. Chong, E. Jorswieck, and G. Fettweis, "Framework for link level energy efficiency optimization with informed transmitter," *IEEE Trans. Wireless Commun.*, vol. 11, no. 8, pp. 2946–2957, Aug. 2012.

[16] R. Cavalcante, S. Stanczak, M. Schubert, A. Eisenlatter, and U. Turke, "Toward energy-efficienct 5G wireless communications technologies," *IEEE Signal Process. Mag.*, vol. 13, no. 11, pp. 24–34, Nov. 2014.

[17] A. Zappone, L. Sanguinetti, G. Bacci, E. Jorswieck, and M. Debbah, "Energy-efficient power control: A look at 5G wireless technologies," *IEEE Trans. Signal Process.*, vol. 64, no. 7, pp. 1668–1683, Jul. 2016.

[18] H. Q. Ngo, E. G. Larsson, and T. L. Marzetta, "Energy and spectral efficiency of very large multiuser MIMO systems," *IEEE Trans. Commun.*, vol. 61, no. 4, pp. 1436–1449, Apr. 2013.

[19] E. Bjornson, L. Sanguinetti, and M. Kountouris, "Deploying dense networks for maximal energy efficiency: Small cells meet massive MIMO," *IEEE J. Sel. Areas. Commun.*, vol. 34, no. 4, pp. 832–847, Apr. 2016.

[20] W. Dinkelbach, "On nonlinear fractional programming," *Management Science*, vol. 13, no. 7, pp. 492–498, Jul. 1967.

[21] S. He, Y. Huang, H. Wang, S. Jin, and L. Yang, "Leakage-aware energy-efficient beamforming for heterogeneous multicell multiuser systems," *IEEE J. Sel. Areas. Commun.*, vol. 32, no. 6, pp. 1268–1281, Jun. 2014.

[22] H. H. Kha, H. D. Tuan, and H. H. Nguyen, "Fast global optimal power allocation in wireless networks by local D.C. programming," *IEEE Trans. Wireless Commun.*, vol. 11, no. 2, pp. 510–515, Feb. 2012.

[23] R. Ramamonjison and V. K. Bhargava, "Energy efficiency maximization framework in cognitive downlink two-tier networks," *IEEE Trans. Wireless Commun.*, vol. 14, no. 3, pp. 1468–1479, Mar. 2015.

[24] J. Tang, D. K. C. So, E. Alsusa, K. A. Hamdi, and A. Shojaeifard, "Resource allocation for energy efficiency optimization in heterogeneous networks," *IEEE J. Sel. Areas. Commun.*, vol. 33, no. 10, pp. 2104–2117, Oct 2015.

[25] H. Q. Ngo, E. G. Larsson, and T. L. Marzetta, "Massive MU-MIMO downlink tdd systems with linear precoding and downlink pilots," in *Proc. IEEE Allerton Conf.*, Oct. 2013, pp. 293–298.

[26] N. Saquib, E. Hossain, L. B. Le, and D. I. Kim, "Interference management in OFDMA femtocell networks: issues and approaches," *IEEE Wireless Commun.*, vol. 19, no. 3, pp. 86–95, Jun. 2012.

[27] A. Abdelnasser, E. Hossain, and D. I. Kim, "Clustering and resource allocation for dense femtocells in a two-tier cellular ofdma network," *IEEE Trans. Wireless Commun.*, vol. 13, no. 3, pp. 1628–1641, Mar. 2014.

[28] D. Gesbert, S. Hanly, H. Huang, S. S. Shitz, O. Simeone, and W. Yu, "Multi-cell MIMO cooperative networks: A new look at interference," *IEEE J. Sel. Areas Commun.*, vol. 28, no. 9, pp. 1380–1408, Dec. 2010.

[29] A. Wiesel, Y. C. Eldar, and S. Shamai, "Linear precoding via conic optimization for fixed MIMO receivers," *IEEE Trans. Signal Process.*, vol. 54, no. 1, pp. 161–176, Jan. 2006.

[30] B. R. Marks and G. P. Wright, "A general inner approximation algorithm for nonconvex mathematical programs," *Operation Research*, vol. 26, no. 4, pp. 681–683, Apr. 1978.

[31] G. Liu, M. Sheng, X. Wang, W. Jiao, Y. Li, and J. Li, "Interference alignment for partially connected downlink MIMO heterogeneous networks," *IEEE Trans. Commun.*, vol. 63, no. 2, pp. 551–564, Feb 2015.

[32] J. G. Andrews, S. Buzzi, W. Choi, S. V. Hanly, A. Lozano, A. C. K. Soong, and J. C. Zhang, "What will 5G be?" *IEEE J. Sel. Areas Commun.*, vol. 32, no. 6, pp. 1065–1082, Jun. 2014.

[33] L. D. Nguyen, H. D. Tuan, and T. Q. Duong, "Energy-efficient signalling in QoS constrained heterogeneous networks," *IEEE Access*, vol. 4, pp. 7958–7966, 2016.

[34] H. Tuy, *Convex Analysis and Global Optimization (second edition)*. Springer, 2016.

Trung Q. Duong (S'05, M'12, SM'13) received his Ph.D. degree in Telecommunications Systems from Blekinge Institute of Technology (BTH), Sweden in 2012. Since 2013, he has joined Queen's University Belfast, UK as a Lecturer (Assistant Professor). His current research interests include small-cell networks, physical layer security, energy-harvesting communications, cognitive relay networks. He is the author or co-author of more than 260 technical papers published in scientific journals (142 articles) and presented at international conferences (121 papers).

Dr. Duong currently serves as an Editor for the IEEE TRANSACTIONS ON WIRELESS COMMUNICATIONS, IEEE TRANSACTIONS ON COMMUNICATIONS, IET COMMUNICATIONS, and a Senior Editor for IEEE COMMUNICATIONS LETTERS. He was awarded the Best Paper Award at the IEEE Vehicular Technology Conference (VTC-Spring) in 2013, IEEE International Conference on Communications (ICC) 2014, and IEEE Global Communications Conference (GLOBECOM) 2016. He is the recipient of prestigious Royal Academy of Engineering Research Fellowship (2016-2021).

Octavia A. Dobre (M'05, SM'07) received the Dipl. Ing. and Ph.D. degrees from Politehnica University of Bucharest (formerly Polytechnic Institute of Bucharest), Romania, in 1991 and 2000, respectively. She was a Royal Society Scholar in 2000 and a Fulbright Scholar in 2001. Between 2002 and 2005, she was with Politehnica University of Bucharest and New Jersey Institute of Technology, USA. In 2005, she joined Memorial University, Canada, where she is currently a Professor and Research Chair. She was a Visiting Professor with Universit de Bretagne Occidentale, France, and Massachusetts Institute of Technology, USA, in 2013. Her research interests include 5G enabling technologies, blind signal identification and parameter estimation techniques, cognitive radio systems, network coding, as well as optical and underwater communications among others. Dr. Dobre serves as the Editor-in-Chief of the IEEE COMMUNICATIONS LETTERS, as well as an Editor of the IEEE SYSTEMS and IEEE COMMUNICATIONS SURVEYS AND TUTORIALS. She was an Editor and a Senior Editor of the IEEE COMMUNICATIONS LETTERS, an Editor of the IEEE TRANSACTIONS ON WIRELESS COMMUNICATIONS and a Guest Editor of other prestigious journals. She served as General Chair, Tutorial Co-Chair, and Technical Co-Chair at numerous conferences. She is the Chair of the IEEE ComSoc Signal Processing and Communications Electronics Technical Committee, as well as a Member-at-Large of the Administrative Committee of the IEEE Instrumentation and Measurement Society. Dr. Dobre is a Fellow of the Engineering Institute of Canada.

Long D. Nguyen was born in Dongnai, Vietnam. He received the B.S. degree in electronics and telecommunication engineering and the M.S. degree in telecommunication engineering from the Ho Chi Minh City University of Technology, Vietnam, in 2013 and 2015, respectively. He is currently pursuing the Ph.D. degree with Queen's University Belfast. His research interests include convex optimization techniques, heterogeneous network, relay networks, and massive MIMO.

H. Vincent Poor (S'72, M'77, SM'82, F'87) received the Ph.D. degree in EECS from Princeton University in 1977. From 1977 until 1990, he was on the faculty of the University of Illinois at Urbana-Champaign. Since 1990 he has been on the faculty at Princeton, where he is currently the Michael Henry Strater University Professor of Electrical Engineering. During 2006 to 2016, he served as Dean of Princetons School of Engineering and Applied Science. He has also held visiting appointments at several other universities, including most recently at Berkeley and Cambridge. His research interests are in the areas of information theory and signal processing, and their applications in wireless networks, energy systems and related fields. Among his publications in these areas is the recent book Information Theoretic Security and Privacy of Information Systems (Cambridge University Press, 2017).

Dr. Poor is a member of the National Academy of Engineering and the National Academy of Sciences, and is a foreign member of the Chinese Academy of Sciences, the Royal Society, and other national and international academies. He received the Marconi and Armstrong Awards of the IEEE Communications Society in 2007 and 2009, respectively. Recent recognition of his work includes the 2017 IEEE Alexander Graham Bell Medal, Honorary Professorships at Peking University and Tsinghua University, both conferred in 2017, and a D.Sc. honoris causa from Syracuse University also awarded in 2017.

Hoang Duong Tuan received the Diploma (Hons.) and Ph.D. degrees in applied mathematics from Odessa State University, Ukraine, in 1987 and 1991, respectively. He spent nine academic years in Japan as an Assistant Professor in the Department of Electronic-Mechanical Engineering, Nagoya University, from 1994 to 1999, and then as an Associate Professor in the Department of Electrical and Computer Engineering, Toyota Technological Institute, Nagoya, from 1999 to 2003. He was a Professor with the School of Electrical Engineering and Telecommunications, University of New South Wales, from 2003 to 2011. He is currently a Professor with the School of Electrical and Data Engineering and a core member of Global Big Data Technologies Centre, University of Technology Sydney. He has been involved in research with the areas of optimization, control, signal processing, wireless communication, and biomedical engineering for more than 20 years.